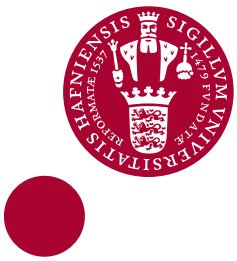

Phylogeny of the hyper-diverse rove beetle subtribe Philonthina with implications for classification of the tribe Staphylinini (Coleoptera: Staphylinidae)

Chani-Posse, Mariana R.; Brunke, Adam James; Chatzimanolis, Stylianos; Schillhammer, Harald; Solodovnikov, Alexey

Published in:
Cladistics

DOI:
10.1111/cla.12188

Publication date:
2018

Document version
Peer reviewed version

Phylogeny of the hyper-diverse rove beetle subtribe Philonthina with implications for classification of the tribe Staphylinini (Coleoptera: Staphylinidae)

M. R. Chani-Posse[1,5*], A. J. Brunke[2,3], S. Chatzimanolis[4], H. Schillhammer[2] and A. Solodovnikov[5*]

1 Laboratorio de Entomología, Instituto Argentino de Investigaciones de las Zonas Aridas (IADIZA, CCT CONICET, Mendoza), Casilla de Correo 507, 5500 Mendoza, Argentina
2 Natural History Museum Vienna, International Research Institute for Entomology, Burgring 7, A -1010, Vienna, Austria
3 Canadian National Collection of Insects, Arachnids and Nematodes, Agriculture and Agri-Food Canada, 960 Carling Avenue, K.W. Neatby Building, Ottawa, K1A 0C6 Ontario, Canada (Current)
4 Department of Biology, Geology and Environmental Science, University of Tennessee at Chattanooga, 615 McCallie Ave., Dept. 2653, Chattanooga, TN, U.S.A.
5 BioSystematics, Natural History Museum of Denmark, Universitetsparken 15, 2100 Copenhagen, Denmark

*corresponding authors: mchani@mendoza-conicet.gob.ar; asolodovnikov@snm.ku.dk

Running head: Reclassification of 'Staphylinini propria'

Abstract

With 71 genera and over 2700 described species, Philonthina is the most speciose subtribe of rove beetle tribe Staphylinini and forms a major component of the largest remaining higher systematics challenge in Staphylinini, the 'Staphylinini propria' clade. A related systematics issue concerns the position of the genus *Holisus* (Hyptiomina), which was recovered within the Neotropical philonthine lineage in several recent analyses of morphology. With the aims of resolving the phylogeny of Philonthina and the position and thus, validity of Hyptiomina, we performed phylogenetic analyses of the tribe Staphylinini based on molecular (six genes, 4471 bp) and morphological (113 characters) data including 138 taxa from all relevant lineages of Staphylinini. We found that 'Staphylinini propria' is a monophylum consisting of six lineages: current subtribes Anisolinina, Philonthina, Staphylinina and Xanthopygina; and two **new subtribes**, Algonina Schillhammer and Brunke and Philothalpina Chatzimanolis and Brunke. While the previously hypothesized Neotropical lineage of Philonthina was corroborated, *Holisus* was recovered as a separate subtribe, outside of Philonthina, within an informal 'Southern Hemisphere clade'. Based on our analyses, we propose tentative new concepts of the polyphyletic genera *Belonuchus* and *Philonthus*. We propose the following taxonomic changes: synonymy of the subtribes Staphylinina Latreille (valid name) and Eucibdelina Sharp; **resurrection of** genera *Barypalpus* Cameron and *Trapeziderus* Motschulsky from synonymy with *Rientis* Sharp and *Belonuchus* Nordmann, respectively; transfer of 38 *Belonuchus* species, 16 *Hesperus* Fauvel species and one *Philonthus* Stephens species to *Trapeziderus* as **new combinations**; transfer of two *Hesperus* species to *Eccoptolonthus* Bernhauer as **new combinations**; transfer of one *Belonuchus* species to *Paederomimus* Sharp as a **new combination**; and transfer of *Pridonius* Blackwelder **new status** from its position as a subgenus of *Quedius* (subtribe Quediina) to Philonthina as a genus, and **new combinations** for its two described species.

Table of Contents

Introduction

The rove beetle tribe Staphylinini is an impressively diverse lineage of predatory insects, occurring in most of the world's terrestrial ecosystems (Brunke *et al.,* 2016). Fossil data, as well as diversity and distribution patterns displayed by extant members of Staphylinini suggest that, although the tribe must have appeared during the Late Jurassic – Early Cretaceous, the most ecologically dominant and diverse crown-groups such as Philonthina are younger (Solodovnikov *et al.*, 2013; Cai *et al.*, 2014; Chani-Posse and Newton, 2015). While phylogenetic relationships reflecting the earlier divergences within this tribe have already been gradually solved in the series of recent papers (Solodovnikov, 2005, 2006; Solodovnikov and Newton, 2005; Solodovnikov and Schomann, 2009; Chatzimanolis *et al.* 2010; Brunke and Solodovnikov 2013; Solodovnikov *et al.* 2013; Brunke *et al.* 2016), the more terminal and speciose branches received less attention. With 71 genera and over 2700 described species, Philonthina is the largest of these younger groups (Newton, unpublished database). Recently, morphology-based phylogenetic analyses of the Oriental and Neotropical groups of Philonthina by Li and Zhou (2011) and Chani-Posse (2013), respectively, as well as the molecular phylogeny of the '*Cafius*-complex' by Jeon *et al.* (2012) have demonstrated how little is known about philonthine evolution and that the supra-generic classification of this group is artificial and inadequate.

Philonthines are predacious both as adults and larvae, hunting their prey mainly in decaying organic matter such as leaf litter, carrion, dung, fungi, rotting fruits, and compost piles (Chani-Posse, 2014a). Philonthina are predominantly tropical and those not found in the tropics are mainly confined to the Northern Hemisphere. Some species of Philonthina display high degrees of specialization, such as an association with microhabitats created by certain plant genera (Frank and Barrera, 2010; Chani-Posse and Couturier, 2012), or with the world's marine littoral habitats in the case of *Cafius* and related genera (Jeon *et al.*, 2012). A number of philonthines such as *Belonuchus docilis* Sharp and *B. stenoderus* Sharp are strongly flattened and adapted to subcortical microhabitats. A final interesting feature of Philonthina is that it is one of a few rove beetle groups outside Aleocharinae, Pselaphinae and Scydmaeninae where myrmecophily has definitively evolved (Parker, 2016). Within the Neotropical members of the subtribe, myrmecophily seems to have evolved at least twice: with army ants of the genus *Eciton* Latreille (Seevers 1965), and with leafcutter ants (Parker, 2016; Chatzimanolis and Chani-Posse, 2016). In spite of its many remarkable features, this highly speciose lineage is currently divided into a number of conventionally defined genera which neither account for such variability, nor reflect the phylogeny of the group. Certainly there is an acute need to improve the systematics of Philonthina in order to make this group accessible to the broader scientific community.

Here we focus on resolving a few larger-scale phylogenetic problems associated with Philonthina. The systematic position of *Holisus*, recently considered to be a philonthine (Solodovnikov and Schomann, 2009; Li and Zhou, 2011; Chani-Posse 2013) has implications for the higher-level systematics of the entire tribe Staphylinini as it is the sole member of subtribe Hyptiomina. The flattened morphology of *Holisus* associated with subcortical life has confused systematists for a long time (Newton 1988). Currently the controversy has become restricted to whether Hyptiomina is a sister lineage to the subtribe Tanygnathinina (Solodovnikov and Newton 2005; Chatzimanolis *et al.* 2010), or whether *Holisus* is a highly derived lineage of Philonthina. These alternatives imply very different biogeographic explanations for the disjunct distribution of *Holisus*, which is mostly confined to the Neotropics, but also includes tropical West Africa based on a single species: *H. schedli* Scheerpeltz, 1956 (Herman, 2001; Newton, unpublished database). Although the generic identity of *H. schedli* has been questioned (Chani-Posse, 2013), the placement of this and two more African *Holisus* species has been recently confirmed (Chani-Posse, pers. obs.). Resolving the position of Hyptiomina is further complicated by the need to consider myrmecophilic Philonthina in addition to subcortical ones because *Holisus* was resolved as sister-group to a myrmecophilous group of genera within the *Belonuchus* complex in Chani-Posse (2013). None of the previous phylogenies have explicitly focused on clarifying the systematic position of *Holisus* and both of the proposed hypotheses have been suspected to be cases of long-branch attraction (Chatzimanolis *et al.* 2010; Chani-Posse 2013).

Another challenge posed by Philonthina is lack of stable and natural generic limits within the subtribe, especially for the recently revealed 'Neotropical lineage' of Philonthina and its most problematic '*Belonuchus* complex' (Chani-Posse, 2013). The genus *Belonuchus* Nordmann, in its current concept, is represented by two different lineages: the 'true *Belonuchus*', including the type species and 186 other New World species; and a second one composed of many Old World species representing the genus

Trapeziderus Motschulsky, a current synonym of *Belonuchus* (Li and Zhou, 2010). In fact, the systematic issues posed by *Belonuchus* are connected to those outlined above for *Holisus* because of the tendency of some *Belonuchus* species to become flattened. Even more problematic genera are the global and species-rich *Philonthus* Stephens, *Bisnius* Stephens, *Gabrius* Stephens and *Hesperus* Fauvel. The non-monophyly of *Philonthus,* a genus with more than 1300 species (Newton, unpublished database), has been largely suspected long ago (Smetana, 1995), especially with respect to the related genera *Bisnius* and *Gabrius.* More recently, morphology-based phylogenies have questioned the monophyly of *Hesperus* (Schillhammer, 2002, 2016; Li and Zhou, 2011) and *Belonuchus* (Chani-Posse, 2013, 2014a). Using molecular data Jeon *et al.* (2012) revealed a conflict between the currently accepted generic limits of the '*Cafius*-complex' and phylogeny. These large para- or polyphyletic genera of Philonthina remain challenging for modern revisionary work and misleading for those who may use rove beetles for estimates of large scale biodiversity patterns.

Given the challenges outlined above, the main goals of our study were: carry out a phylogenetic analysis of Staphylinini using morphological and molecular data with subtribes Philonthina and Hyptiomina as focal points; test the monophyly of the Neotropical lineage (*sensu* Chani-Posse, 2013) of Philonthina, especially its '*Belonuchus* complex'; and test the monophyly and sister group relationships of each of the most speciose genera within Philonthina. The breadth of the *Holisus* problem required the taxon sampling for this paper to broadly cover diversity across Staphylinini. Therefore, secondary aims of our study were: test the recently proposed backbone reclassification of Staphylinini by Brunke *et al.* (2016) with new data; and acquire more insight about the phylogeny of 'Staphylinini propria', including the composition and sister-group relationships of its subtribes Staphylinina, Eucibdelina, Anisolinina, Xanthopygina and Philonthina.

Unlike the previous phylogenetic analyses conducted for the tribe Staphylinini that were either based on morphology or molecular data only, we here performed a combined analysis. Advantages of integrating molecular and morphological datasets in combined analyses have been largely addressed (e.g., Hillis and Wiens, 2000; Wiens, 2004, 2009), as has the importance of complementing alternative data sources in phylogenetics (e.g., Lopardo *et al.*, 2011; Reeder *et al.*, 2015; Sørensen *et al.*, 2015).

Materials and Methods

Taxon selection

In total, 138 taxa were included in the dataset (Table S1) with representatives of each of the seven subtribes recognized by Brunke *et al.* (2016), five subtribes currently composing 'Staphylinini propria', as well as Staphylinini currently *incertae sedis* at the subtribal level. For Philonthina and its Neotropical lineage *sensu* Chani-Posse (2013), representatives of all DNA-grade available genera were included. Four species for which DNA was not available were nevertheless included in the taxon sample, either because their placement in Philonthina was not fully resolved (*Quedius iheringi*) (Brunke *et al.*, 2016), or due to their importance in defining generic limits (*Belonuchus haemorrhoidalis*) or sister group relationships (*Holisus* sp. and *Atanygnathus* sp.). To thoroughly test the hypothesis that Hyptiomina and Tanygnathinina are sister groups, three members of each of the two respective genera (*Holisus* and *Atanygnathus*) were included in the taxon sample. As basal relationships of Staphylinini have been broadly explored and settled by Brunke *et al.* (2016), basal grade lineages were sampled less densely. Among the extant taxa, Arrowinini and Staphylinini are sister groups within the subfamily Staphylininae (Solodovnikov and Newton, 2005; Solodovnikov *et al*., 2013), therefore *Arrowinus minutus* Solodovnikov and Newton was included to root the trees.

Morphological study

External and genitalic morphology was studied using either dry specimens or disarticulated, cleared preparations in glycerin. Observations were made using a Leica MZ APO stereoscope. Glycerin preparation methods were described by Solodovnikov (2006). Photographs were taken using either a Leica DFC 420 camera attached to a Leica MZ16A microscope with the help of Leica Application Suite (Leica Microsystems, 2003-2007) or captured with a Nikon D4 camera in combination with a bellows and a Rodenstock Apo-Rodagon N 50/2.8, the camera tethered to a PC and controlled via Nikon Camera Control Pro. Photomontage was accomplished using Zerene Stacker (Zerene Systems LLC, 2012) and

photos were edited in Adobe Photoshop CS v4/v5.1/v6 (those edited with v4 were extracted with a plug-in named Fluid Mask). Terminology follows that of Smetana and Davies (2000), with further modifications by Solodovnikov and Newton (2005), Brunke and Solodovnikov (2013) and Chani-Posse (2013, 2014a). Specimens used for morphological study were deposited in the following institutions:

FMNH	Field Museum of Natural History, Chicago, Illinois, U.S.A. (M. Thayer, A. Newton)
INBIO	Instituto Nacional de Biodiversidad, Heredia, Costa Rica (A. Solís)
NHM	Natural History Museum, London, United Kingdom (R. Booth)
NMW	Naturhistorisches Museum Wien, Vienna, Austria (H. Schillhammer)
SEMC	Snow Entomological Collection, Natural History Museum/Biodiversity Research Center, University of Kansas, Lawrence, U.S.A (Zachary H. Falin)
ZMHB	Museum fur Naturkunde der Humboldt Universität, Berlin, Germany (Johannes Frisch, Joachim Willers)
ZMUC	Zoological Museum, University of Copenhagen, Copenhagen, Denmark (A. Solodovnikov, S. Selvantharan)

Morphological characters

Selection of characters mainly follows the character system developed by Smetana and Davies (2000), Solodovnikov and Newton (2005), Li and Zhou (2011), Solodovnikov and Schomann (2009), Brunke and Solodovnikov (2013, 2014) and Chani-Posse (2013, 2014ab). A matrix of character states across the 138 terminal taxa as well as character/character-state descriptions prepared with Mesquite version 3.01 (Maddison and Maddison, 2015) is provided (see Supporting information). Among the characters used, 97 were derived from external morphology, 12 from male genitalia, and 4 from female genitalia. Characters are listed below in sections according to their corresponding body parts. Two characters (9 and 105) are parsimony-uninformative, but were retained in the matrix and included in the analyses to make them traceable as potential autapomorphies. All characters were treated as unordered (non-additive). Following Sereno (2007, 2009), neomorphic (presence/ absence) and transformational (transformation from one state to another) characters referring to the same structure were coded separately. Ninety-one characters were included and illustrated in previous studies (see character list below), 22 characters are novel and therefore marked in the character report with an asterisk (*). WinClada v. 1.00.08 (Nixon, 1999) was used for character mapping.

Antennae (characters 1-6)

1. Antennal insertions (ai), position in relation to frontoclypeus and eye: 0. ai situated at the anterior margin of frontoclypeus, i.e., anterior margin of antennal cavity touching the anterior margin of frontoclypeus (Chani-Posse, 2013: figs. 1B, C); 1. ai situated closer to frontoclypeus than to eye (Chani-Posse, 2013: fig. 1A); 2. ai situated at equal distance or closer to eye (Chani-Posse, 2014a: fig. 11D).
2. Antennae, relative length of antennomere 1 (a1), and antennomeres 2 (a2) and 3 (a3) combined: 0. a1 distinctly shorter than a2 and a3 combined; 1. a1 as long as or longer than a2 and a3 combined.
3. Antennae, length of antennomeres 3 and 2 ratio (a3/a2): 0. a3 not longer than a2 (maximum a3/a2 ratio 1.0); 1. a3 moderately longer than a2 (a3/a2 ratio 1.2-1.5); 2. a3 distinctly longer than a2 (a3/a2 ratio >> 1.5).
4. Antennae, antennomere 3, tomentose pubescence (see Chani-Posse, 2014a): 0. absent (fig. 1D); 1. present (fig. 1C).
5. Antennae, antennomere 4, tomentose pubescence: 0. absent; 1. present (Chani-Posse, 2014a: fig. 1D).
6. Antennae, antennomere 6, apical long setae (see Chani-Posse, 2014b): 0. absent (fig. 10); 1. present (fig. 11).

Head and mouthparts (characters 7-30)

7. Head, dorsal surface punctation: 0. not sexually dimorphic (i.e, both male and female with same punctation); 1. sexually dimorphic (i.e., with dense punctation in males, scarcely punctate to almost glabrous in females) (Chani-Posse, 2014b: fig. 12E).
8*. Head, ventral surface punctation: 0. not sexually dimorphic (i.e, both male and female with same punctation); 1. sexually dimorphic (i.e., with dense punctation in males, scarcely punctate to almost glabrous in females).

9. Head, neck constriction: 0. neck distinct at sides only (Solodovnikov and Newton, 2005: figs. 16A-D); 1. neck constriction fully developed, distinct all around (Chani-Posse, 2013: figs. 1A, B, F).
10. Head, dorsal basal ridge (see Li and Zhou, 2011): 0. absent (figs. A, F); 1. present (figs. B-E).
11. Head, ventral basal ridge (vbr), development: 0. vbr along considerable portion of its length confluent with ventral portion of postoccipital suture (Chani-Posse, 2014a: fig. 2I); 1. vbr strongly (to moderately) projecting anteriad (Solodovnikov and Newton, 2005: fig. 2F); 2. vbr extending more or less parallel to ventral portion of postoccipital suture (Chani-Posse, 2013: figs. 3A–D, F).
12. Head, postgenal ridge: 0. absent (Solodovnikov and Newton, 2005: fig. 9D); 1. present (Chani-Posse, 2013: figs. 3A, D, E, F).
13*. Head, postgenal ridge (pgr) relative to ventral basal ridge (vbr), development (see Chani-Posse, 2014a): 0. pgr developed ventrally but not joining vbr medially (fig. 2D); 1. pgr joined vbr medially (figs. 2A-C, I); 2. pgr slightly developed ventrally (rather laterally) and not joining vbr.
14. Head, postmandibular ridge: 0. absent (Chani-Posse, 2014a: fig. 2B); 1. present (Chani-Posse, 2013: figs. 3A–C, F).
15. Head, postmandibular ridge (pmr) relative to mandibular base (mb) (see Chani-Posse, 2013): 0. pmr bordering mb almost completely (figs. 3B, C); 1. pmr bordering mb only laterally (fig. 3A); 2. pmr and mb separate (fig. 3F).
16*. Head, postmandibular sulcus (see Chani-Posse, 2014a): 0. absent (figs. 2B-D, H); 1. present (fig. 2A).
17. Head, infraorbital ridge (see Chani-Posse, 2014a): 0. absent (figs. 2B, D, I); 1. present (figs. 2A, F-H, J, K).
18. Head, infraorbital ridge (ior), development (see Chani-Posse 2014a): 0. ior complete (figs. 2F, K); 1. ior extending far beyond postgenal ridge (figs. 2G, H); 2. ior reaching postgenal ridge or slightly extending beyond postgenal ridge (figs. 2A, J).
19. Head, ligula, shape (see Li and Zhou, 2011): 0. more or less bilobed, with variously developed rounded lobes (figs. 7C); 1. small, entire (or at most slightly notched medially) (figs. 7A, B); 2. strongly reduced, indistinct.

Note: Li and Zhou (2011) has interpreted fig. 7D (*Erichsonius* sp. 1) as “more or less bilobed”. Herein we consider that the condition shown by the species of *Erichsonius* is not homologous to the so-called bilobed ligula but to the small, entire and slightly notched ligula, and as such has been scored in the present study.

20. Head, mandibles, dorso-lateral groove: 0. absent; 1. present (Chani-Posse, 2013: fig. 1A).
21. Head, mentum, seta alpha (see Brunke and Solodovnikov, 2013): 0. absent (fig. 7C); 1. present (figs. 7A, B).
22. Labial palpus, palpomere 2 (preapical), setal brush: 0. absent; 1. present (Brunke *et al.*, 2016: fig. 5C).
23. Labial palpus, palpomere 3 (apical), shape: 0. subacute, i.e., narrowed at base and evenly converging towards apex (Li and Zhou, 2011: figs. 8B-D); 1. fusiform to apically expanded, i.e., narrowed at base but not (or not evenly) converging towards apex (Li and Zhou, 2011: figs. 8A, E, F); 2. subcylindrical "rod-like", parallel-sided at most of its length, apex subtruncate (Chani-Posse, 2013: fig. 1H); 3. extremely elongate (like in *Atanygnathus*).
24. Labial palpus, relative length of palpomeres 3 (p3, apical) and 2 (p2, preapical) (p3/p2): 0. p3 distinctly shorter than p2; 1. p3 and p2 subequal in length; 2. p3 distinctly longer than p2.
25. Maxillary palpus, palpomere 4 (apical), shape: 0. subacute, i.e., narrowed at base and evenly converging towards apex (Li and Zhou, 2011: figs. 6A, C); 1. fusiform to expanded apically, i.e., narrowed at base but not (or not evenly) converging towards apex (Li and Zhou, 2011: figs. 6D, F); 2. subcylindrical "rod-like", parallel-sided at most of its length, apex subtruncate (Chani-Posse, 2013: fig. 1A); 3. subcylindrical "rod-like", parallel-sided at most of its length, apex acute (Chani-Posse, 2013: fig. 1C); 4 extremely elongate (like in *Atanygnathus*).
26. Gular sutures (gs), development (see Chani-Posse, 2013): 0. gs joined before neck (figs. 3A, D, E); 1. gs not joined before neck, extended close to each other at base of head capsule (figs. 3B, C, F).
27*. Gular sutures (gs), if not joined before neck, degree of separation: 0. gs slightly separated from each other (Chani-Posse, 2013; figs. 3B, C, F); 1. gs widely separated from each other.
28*. Gular sutures, if joined before neck, meeting (see Chani-Posse, 2013): 0. anteriorly (i.e., not farther than one half the distance between the anterior margin of mentum and the base of head along midline) (figs. 3A, E); 1. posteriorly (fig. 3D).
29*. Hypostomal cavity (hc): 0. absent; 1. present (Smetana and Davies, 2000: figs. 8, 10).
30*. Hypostomal cavity (hc), if present: 0. hc distinctly delimited (i.e., cavity surface with microsculpture and/or punctation different from rest of nearby head surface); 1. hc moderately delimited (i.e., cavity

surface without microsculpture or punctation different from rest of nearby head surface); 2. hc slightly delimited (cavity distinct only laterally, its surface with same microsculpture or punctation as rest of nearby head surface).

Note: the term "hypostomal cavity" is used after Naomi (1987a,b) where the ventral area of head immediately behind the mandibular insertion is considered the "hypostoma" and delimited by a "hypostomal suture", which has been interpreted as a ridge or "crassa" by Blackwelder (1936). We have not found further references to this structure.

Neck (characters 31, 32)

31. Neck, transverse carina: 0. absent; 1. present (Chani-Posse, 2013; fig. 1A).
32. Neck, disc punctation (i.e., coarser than microscopic micropunctulation on dorsal surface of neck and not including dorsolateral areas): 0. absent (Smetana and Davies, 2000: fig. 39); 1. distinct (Li and Zhou, 2011: fig. 3C).

Note: the term "micropunctulation" is used after Smetana and Davies (2000).

Prothorax (characters 33-51)

33. Prothorax, anterior angles (aap) relative to anterior margin of prosternum (amp) (see Chani-Posse, 2013): 0. aap not strongly produced beyond amp (fig. 2C); 1. aap strongly produced beyond amp (fig. 1N).
34*. Prothorax, pronotum, long marginal setae: 0. distinct, regularly distributed; 1. not distinct and not regularly distributed.
35. Prothorax, large lateral setiferous puncture (llsp), position in relation to superior marginal line of pronotum (smlp) (see Chani-Posse, 2014a): 0. llsp situated very close to smlp or at a distance no more than three times its diameter (fig. 4F); 1. llsp situated away from smlp at a distance at least three times as large as its diameter (figs. 4G–I).
36. Prothorax, pronotum, punctation of disc (see Chani-Posse, 2014a): 0. coarse (fig. 4H); 1. fine (figs. 4E-G, I-K).
37. Prothorax, basisternum (bs), length relative to length of furcasternum (fs) (bs/fs, measured laterally): 0. bs slightly to moderately longer than fs (bs/fs ratio up to 1.5); 1. bs distinctly longer than fs (bs/fs ratio >> 1.5); 2. bs distinctly shorter than fs (bs/fs ratio <<1.0)
38. Prothorax, prosternum, transverse carina on basisternum: 0. absent; 1. present (Chani-Posse, 2013: figs. 1N, 2D).
39. Prothorax, prosternum, transverse carina on basisternum (tc), development (when present): 0. tc rudimentary to uncomplete; 1. tc complete (Chani-Posse, 2013: figs. 1N, 2D).
40*. Prothorax, prosternum, transverse carina on basisternum (tc), shape (when present): 0. tc straight; 1. tc distinctly acute medially.
41. Prothorax, prosternum, longitudinal ridge (in ventral view) (see Li and Zhou, 2011): 0. absent (figs. 11D, F); 1. present (figs. 11A-C, E).
42. Prosternum, keel (see Chani-Posse and Asenjo, 2013): 0. absent (fig. 2J); 1. present (figs. 2H, I).
43. Prothorax, prosternum, microsculpture of oblique and transverse waves: 0. faint on both basisternum and furcasternum; 1. faint on basisternum, distinct on furcasternum; 2. distinct on basisternum, faint on furcasternum.
44*. Prothorax, prosternum, furcasternum, meshed microsculpture: 0. absent; 1. present.
45. Prothorax, hypomeron, superior marginal line, deflection under anterior angles (ventral view): 0. not distinct; 1. distinct (Chani-Posse, 2013: figs. 1A-D).
46. Prothorax, hypomeron, inferior marginal line (iml), development (see Smetana and Davies, 2000): 0. iml not continued as a separate entity beyond anterior pronotal angles (figs. 42-44); 1. iml continued as a separate entity beyond anterior pronotal angles and curving around them (fig. 53); 2. iml continued as a separate entity beyond anterior pronotal angles and continuous with them (fig. 49).
47. Prothorax, postcoxal process (see Li and Zhou, 2011): 0. absent (figs. 10A, D); 1. present (figs. 10B, C).
48. Prothorax, degree of fusion of pronotum (pnt) and prosternum (pst) (see Li and Zhou, 2011): 0. pnt and pst not fused in procoxal cavity, pronotosternal suture complete in cavity (fig. 10C); 1. pnt and pst at least partially fused, pronotosternal suture missing in part of cavity (figs. 10A-D).
49. Prothorax, prosternum, basisternum, pair of macrosetae: 0. absent; 1. present (Smetana and Davies, 2000: fig. 86).

50*. Prothorax, prosternum, basisternum, position of pair of macrosetae (ms, if present) in relation to anterior margin of prosternum (amp) and the sternacostal suture (ss): 0. ms situated close to amp (i.e., not farther than one fourth the distance between amp and the ss along midline) (Smetana and Davies, 2000: fig. 86); 1. ms situated far from amp (i.e., farther than one fourth the distance between amp and the ss along midline) (Li and Zhou, 2011: figs. 11A, B, E, F).

Mesothorax including elytra (characters 51-64)

51. Mesothorax, elytron, subbasal ridge (see Brunke and Solodovnikov, 2013): 0. absent (fig. 8E); 1. present (figs. 8A-D, F).
52. Mesothorax, elytron, subbasal ridge (sbr), shape (see Brunke and Solodovnikov, 2013): 0. sbr horizontal, reaching humerus (figs. 8A,B); 1. sbr horizontal but reduced, not reaching humerus (fig. 8C); 2. sbr sinuate, directed anteriad (fig. 8F).
53. Mesothorax, mesoscutellum, posterior scutellar ridge (see Brunke and Solodovnikov, 2013): 0. absent (figs. 8A,C, D, E); 1. present (figs. 8B, F).
54. Mesothorax, elytron, humeral spines or spine-like setae: 0. absent; 1. present (Brunke and Solodovnikov, 2014: figs. 10B-E).
55. Mesothorax, elytron, punctation of epipleuron: 0. absent; 1. consists of a few macrosetae arranged in a row (Brunke *et al.*, 2016, figs. 4a-c); 2. with even punctation.
56. Sternopleural (anapleural) suture (see Chani-Posse, 2014a): 0. transverse, or nearly transverse (very slightly oblique) (fig. 8B); 1. distinctly oblique (medial end of suture anterior to its lateral end) (fig. 8C); 2. sinuate (fig. 8A).
57*. Sternopleural (anapleural) sutures (sps), their position with respect to anterior margin of mesoventrite (amm): 0. sps confluent at amm; 1. sps not confluent at amm
58. Mesothorax, mesoventral anterior carina of prepectus: 0. absent; 1. present.
59*. Mesothorax, mesoventral anterior half of prepectus, free (not connected) ridge: 0. absent; 1. present (Chani-Posse, 2014a: fig. 2B).
60*. Mesothorax, mesoventral posterior half of prepectus, ridge connecting coxal cavities: 0. absent; 1. present (Li and Zhou, 2011: figs. 12E; Smetana and Davies, 2000: fig. 87).
61*. Mesothorax, mesoventral posterior half of prepectus, ridge connecting coxal cavities, if present: 0. straight to slightly arcuate (Li and Zhou, 2011: fig. 12E); 1. distinctly arcuate to obtuse (Smetana and Davies, 2000: fig. 87).
62*. Mesothorax, mesoventral posterior half of prepectus, acute ridge not connecting coxal cavities: 0. absent; 1. present (Li and Zhou, 2011: fig. 12C).
63. Mesothorax, mesocoxae (see Smetana and Davies, 2000): 0. distinctly recessed compared to metaventrite and intercoxal process, mesocoxae therefore contiguous (fig. 158); 1. distinctly recessed compared to metaventrite but on approximately same plane as intercoxal process, mesocoxae therefore moderately separated (fig. 87); 2. not distinctly recessed, on approximately same plane as intercoxal process and metaventrite, mesocoxae therefore at least narrowly separated (fig. 117).
64. Mesothorax, intercoxal process, apex: 0. rounded or broadly pointed, forming obtuse angle (Chani-Posse, 2014a: fig. 2B); 1. narrowly pointed forming sharp (acute) angle (Li and Zhou, 2011: figs. 12B-F); 2. distinctly truncate; 3. intercoxal process not distinct, metaventrite fused with mesoventrite (Li and Zhou, 2011: fig. 12A).

Legs (characters 65-79)

65. Protibiae, shape (see Chani-Posse, 2014a): 0. cylindrical to slightly broadened apically (figs. 6B-D); 1. subconical, moderately broadened apically (figs. 7F, G); 2. conical, distinctly broadened apically; 3. distinctly broadened and flattened laterally.
66*. Protibiae, apical excavation: 0. absent; 1. present.
67*. Profemora, lateroventral medial spines (posterior row): 0. absent; 1. present.
68*. Profemora, lateroventral apical spines (anterior row): 0. absent; 1. present.
69. Protarsi, shape of tarsomeres 1-4 (see Chani-Posse, 2014a): 0. more or less cylindrical, not transversely widened and not flattened dorso-ventrally (fig. 6C); 1. more or less flattened dorso-ventrally and widened distally (figs. 7F, G); 2. more or less flattened dorso-ventrally but not widened distally (figs. 7D, E).
70. Protarsi, ventral chaetotaxy, modified pale (adhesive) setae: 0. absent; 1. present (Li and Zhou, 2011: figs. 16A, B).
71. Metacoxae, transverse carina: 0. absent; 1. present (Li and Zhou, 2011: fig. 16C).
72*. Metacoxae, ventral spines: 0. absent; 1. present.

73. Male metafemora, spines: 0. absent; 1. present.
74. Metatarsi, relative length of tarsomeres 1 (t1) and 5 (t5) (t1/t5): 0. t1 shorter than t5 or at most both tarsomeres subequal (t1/t5 < 1.0); 1. t1 moderately longer than t5 (t1/t5 >> 1.0 but < 2.0); 2. t1 significantly longer than t5 (t1/t5 >> 2.0 but < 3.0); 3. t1 much longer than t5 (t1/t5 = 4.0).
75. Metatarsi, tarsomeres 3-5, dorsal surface, chaetotaxy: 0. developed only at margins, dorsal surface of tarsomeres glabrous along midline; 1. tarsomeres dorsally setose (setae not restricted to marginal series).
76. Metarsi, tarsomere 4, inner marginal spine-like setae (see Brunke and Solodovnikov, 2013): 0. absent (fig. 9A); 1. present (fig. 9B).
77. Metatibiae, spines: 0. absent, or at most one or two spines present; 1. always several spines present.
78. Apical tarsomere, empodial setae (see Smetana and Davies, 2000): 0. absent (figs. 70, 71); 1. present (figs. 67-69).
79. Apical tarsomere, empodial spine: 0. absent; 1. present (Chani-Posse, 2013: fig. 2G).

Hind wings (characters 80, 81)

80. Hind wing, venation, veins CuA and MP4: 0. completely separate (Brunke and Solodovnikov, 2014: fig. 9A); 1. fused in one vein (although often its origin from two veins still very obvious) (Chani-Posse, 2013: fig. 4A).
81. Hind wing, venation, MP3: 0. vein MP3 present, although sometimes faint (Brunke and Solodovnikov, 2014: fig. 9A); 1. vein MP3 absent.

Abdomen (characters 82-95)

82. Abdomen, prototergal glands, cuticular manifestation (see Li and Zhou, 2011): 0. shallow impression; 1. well-developed acetabula (fig. 17C); 2. more or less invaginated capsules with smaller openings (fig. 17A, B).
83. Abdomen, shape (see Chani-Posse, 2013): 0. flattened dorsoventrally (fig. 5A); 1. conical (fig. 5B); 2. subcylindrical (fig. 5C); 3. subconical (fig. 5D).
84. Abdomen, terga 3 and 4, anterior basal transverse carina (ABTC), pair of accessory ridges: 0. absent; 1. present.
85. Abdomen, tergum 3, posterior basal transverse carina (PBTC): 0. absent; 1. present.
86. Abdomen, tergum 5, ABTC, pair of accessory ridges: 0. absent; 1. present.
87. Abdomen, tergum 4, PBTC: 0. absent; 1. present.
88. Abdomen, tergum 5, PBTC: 0. absent; 1. present.
89. Abdomen, tergum 5, PBTC, shape (if present): 0. pl straight or acutely pointed medially; 1. pl broadly arcuate.
90. Abdomen, tergum 3, curved ridge on disc: 0. absent; 1. present.
91. Abdomen, tergum 4, curved ridge on disc: 0. absent; 1. present.
92. Abdomen, tergum 5, curved ridge on disc: 0. absent; 1. present.
93. Abdomen, sternum 3, basal transverse carina, medial area (see Li and Zhou, 2011): 0. straight to arcuate (fig. 18C); 1. acutely pointed medially (figs. 18A, D); 2. angulate medially (fig. 18B).
94. Abdomen, sternum 3, basal transverse carina, shape of its lateral area: 0. not sinuate; 1. sinuate.
95. Abdomen, male sternum 7, patches of setae on disc: 0. absent; 1. present (Schillhammer, 2004b: figs. 12-13).

Genitalia and associated structures (characters 96-113)

96. Male sternum 8, apical margin, distinct medial projection: 0. absent; 1. present (Chani-Posse, 2014b: figs. 21, 30, 47, 51, 59).
97. Female sternum 8, apical margin, distinct medial projection: 0. absent; 1. present (Chani-Posse, 2014b: figs. 26, 35, 56).
98. Male sternum 9, relative length of basal (bp) and distal (dp) portions (bp/dp): 0. bp shorter or as long as dp at most (bp/dp 1.0); 1. bp moderately longer than dp (bp/dp 1.2-1.4); 2 bp distinctly longer than dp (bp/dp at least 1.6).
99. Male sternum 9, basal portion: 0. more or less symmetrical (i.e., both lateral ends similarly produced, not extending far from each other); 1. asymmetrical (i.e., one lateral end distinctly produced, extending far from the other).
100. Male sternum 9, basal portion, asymmetry: 0. strong (Chani-Posse, 2014b: figs. 22, 31, 39, 48, 52, 60); 1. moderate; 2. slight.
101. Male sternum 9, distal portion, median emargination: 0. distinct; 1. not distinct.

102. Male sternum 9, distal portion, emargination (if distinct): 0. acute (Chani-Posse and Asenjo, 2013: e.g., figs. 3B, F, L, R); 1. subangulate to concave (Chani-Posse, 2014b: figs. 22, 31, 39, 48, 52, 60).
103*. Lateral tergal sclerites 9 (styli), apical straight setae: 0. absent; 1. present.
104. Lateral tergal sclerites 9 (styli), shape: 0. dorsoventrally flattened (Chani-Posse, 2014b: figs. 19, 20); 1. not dorsoventrally or laterally flattened; 2. laterally flattened.
105. Lateral tergal sclerites 9 (styli) (if dorsoventrally flattened): 0. not sexually dimorphic (i.e., equally wide in both male and female); 1. sexually dimorphic (i.e., distinctly wider in males than in females) (Chani-Posse, 2014b: figs. 19, 20).
106. Male tergum 10, shape: 0. emarginate medio-apically; 1. apically subtruncate to wide and subangulate or arcuate; 2. concave medio-apically to apically truncate; 3. apically distinctly subacute to acute.
107. Female tergum 10, apex: 0. subacute; 1. subtruncate apically to wide and subangulate or arcuate apically; 2. truncate to concave; 3. acute.
108. Male: aedeagus, parameres, separation: 0. paired, well separated; 1. fused into a single lobe (sometimes secondarily bifurcate).
109. Male: aedeagus, paramere(s), sensory peg setae: 0. absent; 1. present.
110. Male: aedeagus, paramere(s), degree of attachment to median lobe: 0. fused to median lobe only at base, otherwise paramere(s) distinctly separated from median lobe along entire length; 1. fused to median lobe only at base and very closely appressed to median lobe along entire length; 2. fused to median lobe along its (their) entire length, paramere(s) and median lobe hardly distinguishable from each other.
111. Male: aedeagus, paramere(s), shape: 0. paramere(s) not (or at most slightly) produced over apex of median lobe; 1. paramere strongly produced over apex of median lobe; 2. paramere distinctly small (short and/or thin).
112. Ovipositor, each second gonocoxite, number of macrosetae: 0. 2-5; 1. one at midline.
113*. Female genitalia, accessory sclerite: 0. absent; 1. present.

DNA extraction, amplification, and sequencing

Protocols for DNA extraction and voucher preparation follow those described by Brunke *et al.* (2016). For the extractions performed at UTC, vouchers were treated as in Chatzimanolis (2014). Vouchers of extracted specimens were deposited in either The Natural History Museum of Denmark (ZMUC), University of Tennessee at Chattanooga (UTCI) or The Natural History Museum of Oslo (ZMUN) (see Table S1).

Six gene fragments were selected for phylogenetic inference based on their performance at deep and shallow divergences within Coleoptera (Wild and Maddison 2008), or Staphylininae (Chatzimanolis *et al.* 2010; Chatzimanolis 2014) and to make our study maximally compatible with Brunke *et al.* (2016). We amplified fragments of the nuclear protein encoding genes *carbamoyl-phosphate synthetase* (CAD), *topoisomerase I*, *arginine kinase*, *wingless*, mitochondrial protein encoding *COI*, and nuclear ribosomal *28S*.

In most cases, PCR was accomplished in 25 µl reaction volumes containing 5µl of DNA extract and (all Applied Biosystems): 2.5mM $MgCl_2$, 1X PCR buffer II, 0.5µM of each primer, 0.8mM dNTP mix, 1U of AmpliTaq DNA Polymerase. For difficult amplifications Gold AmpliTaq and 1µl of BSA were used. For reactions performed at UTC (vouchers stored at UTCI) see Chatzimanolis (2014) for details. *Topoisomerase I* and *28S* were amplified as described in Chatzimanolis *et al.* (2010), and *arginine kinase* was amplified as in Chatzimanolis (2014). For difficult 28S amplifications, 1.25µl of DMSO was added instead of Q solution for some taxa. The amplification profile for COI consisted of an initial denaturation for 5 min at 94° C, 35 cycles of: 45 s at 94° C, 30 s at 52° C and 1.5 min at 72° C; followed by a 7 min final extension at 72° C. The amplification profile for Wg using the external primers consisted of an initial denaturation for 2 min at 94° C, 35 cycles of: 1 min at 94 ° C, 30 s at 53° C and 50 s at 72° C; followed by a 5 min final extension at 72° C. The PCR profile for the internal primers was the same as above. For CAD, we followed Brunke *et al.* (2016) on targeting an upstream fragment of ~620 bp and a downstream fragment of ~640 bp, corresponding to 'CADA' and 'CADC' of Chatzimanolis (2014), respectively. Both CADA and CADC were not straightforward to obtain in the present study, so we have followed a nested protocol with different amplification profiles using two DNA polymerases (Gold AmpliTaq or Red AmpliTaq) and several primers (see Table S2). For CADA, PCR was performed following a 'touch-down' like protocol for the external reaction and a regular protocol for the internal reaction, both using Gold AmpliTaq or, alternatively, a regular protocol (external reaction), and a protocol of two annealing stages (internal reaction) using Red AmpliTaq. Working with Gold AmpliTaq, the amplification profile for CADA using the external primers consisted of an initial denaturation at 94°C

for 5 min; 10 cycles of 94°C for 30 s, 57°C for 30 s and 72°C for 2.5 min; 10 cycles of 94°C for 30 s, 52°C for 30 s and 72°C for 2.5 min; 20 cycles of 94°C for 30 s, 45°C for 30 s and 72°C for 2.5 min; and a final elongation step of 72°C for 10 min; the amplification profile using the internal primers consisted of an initial denaturation at 94°C for 5 min; 35 cycles of 94°C for 45 s, 52°C for 30 s and 72°C for 1.5 min; and a final elongation step of 72°C for 7 min. Working with Red AmpliTaq, the amplification profile for both CADA and CADC using the external primers consisted of an initial denaturation at 94°C for 1 min; 35 cycles of 94°C for 45 s, 55°C for 45 s and 72°C for 3 min; and a final elongation step of 72°C for 10 min; the amplification profile using the internal primers consisted of an initial denaturation at 94°C for 1 min; 7 cycles of 94°C for 45 s, 52°C for 45 s and 72°C for 3.5 min; 27 cycles of 94°C for 45 s, 52°C for 45 s and 72°C for 1.5 min; and a final elongation step of 72°C for 7 min. Complete primer details are given in Table S2. Sequencing was performed in both directions by Macrogen Europe (Netherlands).

Sequence assembly, management and alignment

Sequences were edited and assembled in Geneious v7.0.6 (Biomatters Ltd.). GenBank accession numbers of all sequences are given in Table S1. Sequences were aligned using the MAFFT plugin v.7.017 in Geneious, based on MAFFT (Katoh *et al.*, 2002). Protein encoding genes were unambiguously aligned due to few gaps and their codon-based structure. 28S was aligned using the E-INS-i algorithm of MAFFT and ambiguously aligned regions were identified and removed with the server version of Gblocks (Talavera and Castresana, 2007). The default, conservative settings of Gblocks were used, with only 'do not allow many contiguous non-conserved positions' selected, though gaps were allowed in the alignment. The resulting 28S alignment was 622 bp and had only two single nucleotide gaps in *Rhyncocheilus rugilipennis* Cameron. Individual gene alignments were concatenated with the 'concatenate' function of Geneious.

Phylogenetic analyses

A combined matrix of molecular (4458 bp) and morphological (113 characters) data for the total amount of taxa under study (138) was analysed by means of Maximum Parsimony (MP), Maximum Likelihood (ML) and Bayesian Inference (BI). Molecular and morphological data were also analysed separately in order to account for differences in resolution between the two different datasets. While the molecular matrix was analysed by all three methods, the morphological dataset alone was only tested by MP following Assis (2015) and O´Reilly *et al.* (2016). Gaps were treated as missing data in all analyses to allow comparisons between the inference methods.

Maximum Parsimony analyses were conducted in TNT 1.1 (Goloboff *et al.*, 2008b). Driven tree searches were performed using all search methods under 'New Technologies', 'init. level' = 100 (14 additional addseqs) and 'find min. length' = 10. Parsimony analyses were explored with same search strategies under equal weights (EW) and implied weights (IW). The latter was aimed to minimize the effect of homoplasy over phylogenetic signal (Goloboff *et al.*, 2008a) in our mostly protein encoding gene dataset in order to gain in resolution at deeper level divergences (Brunke *et al.*, 2016). In the IW analysis, we changed the constant of concavity K from 6 to 60 (from strong to weak down-weighting of homoplastic changes), and evaluated the recovery of main lineages and groups under its different values. Clade support under EW and IW was assessed by jackknife frequencies and symmetric resampling, respectively (Goloboff *et al.*, 2003). Given the size of the dataset and to speed up the analyses, a traditional search strategy was used for the support estimation. We performed 1000 pseudoreplicates with heuristic searches consisting of ten random addition sequences, followed by ten iterations of tree bisection and reconnection, and holding one tree.

For model-based analyses, the alignments were initially partitioned by gene and, for protein-encoding genes, by position. The optimal partitioning scheme and the corresponding models of nucleotide evolution were determined by PartitionFinder v1.1.0 (Lanfear *et al.*, 2012) using the Bayesian Information Criterion. All models were considered, branch lengths were unlinked and the search was set to the 'greedy' algorithm. Morphological data into the combined matrix were analysed in a single partition using the maximum likelihood model for discrete morphological character data, under the assumption that only characters that varied among taxa were included (MKv) (Lewis, 2001).

Bayesian analyses were conducted in MrBayes v3.2.2 (Ronquist *et al.*, 2012) running on the CIPRES Science Gateway v3.3. (phylo.org). Convergence was visualized in Tracer v1.6 (Rambaut *et al.*, 2014), and by examining PSRF values and the average standard deviation of split frequencies (ASDSF) in the MrBayes output. Bayesian inference was based on two different analyses due to difficulties in getting

values below 0.01 of the average standard deviation of split frequencies for the combined analysis including the 138 taxa. At first, analysis was run on the same combined matrix as that used for MP and ML (138 taxa and 4571 characters). After several trials increasing the number of chains (from 4 to 8), the length of the run (up to 120 million generations) and adjusting heating parameters (from 0.01 to 0.1) in accordance with the mixing behaviour of the chains, an average standard deviation of 0.027 was the lowest ASDSF value reached. Each run consisted of 1 cold and 7 heated chains, ran for 120 million generations and was repeated twice. Prior settings were those used by Brunke *et al.* (2016), except the heating parameter (temp=0.01). It has been said that retention of taxa with high percentage of missing data ('incomplete taxa', with only 5% to 25% data available) can potentially improve phylogenetic accuracy when using model-based methods (Wiens, 2005). In the present study we suspected a detrimental effect on convergence by taxa which were less than 5% complete. Therefore another analysis was run after removing those taxa with only morphological data available (five taxa, ca. 2.5 % complete). This second analysis was performed on a combined matrix including 133 taxa and all conditions were the same as those in the first analysis, except the heating parameter (temp=0.03) and number of generations (30 million); an ASDSF of 0.004 was reached.

Maximum likelihood analysis was performed using the GARLI 2.0 web service (molecularevolution.org) (Bazinet *et al.*, 2014), with default settings, the adaptive search set to 10 (default) and 'infer overall rate multipliers for each data subset' selected. The adaptive search begins with 10 replicates and then, based on the likelihood distribution of the 10 highest likelihood trees found, estimates the number of replicates needed to find the globally most likely tree with 95% probability (Bazinet *et al.*, 2014). Additional replicates are automatically performed if deemed necessary. Node support was assessed by performing 1000 bootstrap pseudoreplicates using the GARLI web service.

Nodes with Bayesian posterior probability (PP) > 0.95 or Parsimony Jackknife (JK)/Symmetric resampling (SR)/Maximum Likelihood Bootstrap (BS) values greater than 80 were considered strongly supported. Nodes with PP = 0.90-0.94 or JK/SR/BS = 70-80 were considered moderately supported. Nodes with PP = 0.81-0.89 or JK/SR/BS = 50-69 were considered to be weakly supported. Nodes with less than 0.81 PP or 50 JK/SR/BS were considered to be unsupported and were generally not included in discussions of topological differences between methods or when discussing monophyly. This categorical treatment of support values helps to group nodes of relatively high support and relatively low support, and represents the general tendency of PP to be less conservative than BS (Erixon *et al.*, 2003).

Character optimization

Character optimization of the most parsimonious trees (MPTs) was obtained from each analysis (EW and IW) using the option "list common synapomorphies" in TNT. Following Simmons and Randle (2014), character changes were also parsimony-optimized in TNT on the ML topology (very similar to BI, see Results) to identify nodes which may be not unequivocally supported by synapomorphies. Synapomorphies from both analyses (MP and ML) were listed for basal nodes and major lineages. The contribution of each gene to molecular synapomorphies as well as the number of morphological synapomorphies supporting each of those nodes were examined and discussed as evidence of support (either ambiguous or unambiguous) and as diagnostic characters for the main clades. Morphological synapomorphies were error-checked and visualized in Mesquite v3.01 (Maddison and Maddison, 2015), using the 'trace all characters' function under the Analysis: Tree menu.

Long-branch attraction

To explore whether previous hypotheses about the sister group of *Holisus* (Hyptiomina) were cases of long-branch attraction (LBA), we followed the recommendations of Bergsten (2005) including: increasing the size of both the taxon sample and data to be analysed, partitioned analyses, long branch extraction and/or outgroup replacement, as well as analysing data by means of different methodologies. The current matrix represents the largest and most complete dataset for Staphylinini known to date. Both model-based (MB and ML) and MP analyses were run for the combined and partitioned (DNA vs. morphology) datasets. Afterwards, taxa suspected of promoting LBA were extracted from the combined dataset and the position of the putative remaining counterpart (representatives of *Holisus*) was tested by parsimony under this new framework.

Results

Combined dataset

The combined dataset for 138 taxa was 4571 characters in length (4458 bp and 113 morphological characters) and contained 19.5% missing data (see Supporting information). It included three taxa for which only molecular data was available (*Atanygnathus acuminatus*, *Holisus* sp. from Costa Rica and *Neobisnius occidentoides*) and four taxa with only morphological data available (*Quedius iheringi*, *Belonuchus haemorrhoidalis, Holisus* sp. from Ecuador, and *Atanygnathus* sp.).

Molecular dataset

The resulting concatenated alignment (133 taxa) was 4458 bp in length and contained 20% missing data. It included at least four of the six genes considered herein for each taxon, with exception of four taxa (*Philonthus caeruleipennis*, *Bisnius sordidus*, *Belonuchus* sp. 2 and *Paederomimus cribratus*) where only three genes could be amplified (ca. 40% completeness, see Table S1).

The individual gene alignments for ArgK and both portions of CAD (CADA and CADC) contained no gaps. Apomorphic codon deletions were observed in the TP alignment for the following species: *Bisnius blandus* (one), *Belonuchus* sp. 2 (six) and the three species of *Neobisnius* (two). A single codon deletion occurred twice, approximately halfway in the 28s alignment in *Rhyncocheilus rugilipennis*. The CO1 alignment contained gaps in two species: two deletions (6bp and 9 bp) were discovered close to each other at approximately halfway in *Belonuchus pollens*, and one deletion (6bp) occurred slightly upstream in *Bisnius blandus*. In general, the alignments of Wg contained few gaps but several of these gaps were shared by taxa grouped by previous phylogenetic hypotheses (Brunke *et al.*, 2016) and are also described here. The Wg alignment contained one single codon insertion in all Amblyopinina; one single codon deletion shared by all Tanygnathinina and *Holisus*; and one single codon deletion shared by *Gabronthus flavicollis*, the three species of *Neobisnius*, several *Philonthus* species and *Taxiplagus* sp. The partitioning scheme and corresponding models selected by PartitionFinder were: i) 28S, and positions 1+2 of ArgK, CO1, CAD, TP, and Wg – SYM+I+G; ii) position 3 of ArgK, CAD, TP and Wg – K80+I+G; iii) position 3 of CO1 – GTR+G.

Morphological dataset

The morphological matrix contained 135 informative taxa and 113 characters, including ca. 7% missing data (see Supporting information). The three taxa for which only molecular data was available were not included in the only morphology based analysis (*Atanygnathus acuminatus*, *Holisus* sp. and *Neobisnius occidentoides*).

Combined analyses

All analyses resulted in very similar topologies and here we use the tree from the BI analysis of the combined dataset including 138 taxa to summarize the results (Fig. 1). The strict consensus of the 23 most parsimonious trees (MPTs) under EW and the most likely tree found by GARLI are shown in Fig. 2. Concerning the MP analyses under IW, the strict consensus trees of the MPTs found for the different values of K from K=6 to K=60 did not differ in topology and showed more congruence with the model-based topologies than the strict consensus performed under EW (Fig. 2). The BI analysis including all taxa (138) showed rather low posterior probabilities (PP= 0.81–0.88) for the backbone nodes (Fig. 1) in contrast to the high posterior probabilities (PP= 0.99–1.0) shown by the BI analysis where taxa with more than 95% missing data were pruned. This was in agreement with the rather high support values shown by both ML and MP analyses for those nodes, even including these incomplete taxa. Overall, the consensus topologies recovered by MP, ML and BI analysis were moderately to well resolved, with more backbone nodes being supported in BI and ML analyses (12 and 10 respectively) than in MP (7) (Figs. 1-2). All phylogenetic inference methods were highly congruent in their resultant topologies suggesting strong and consistent signal in the data. Topological incongruences between methods were few, but occurred at both above and below subtribal level, where in most cases conflictive clades were only supported by BI analysis while others were unsupported in all the three methods. Therefore, supported topological congruence between methods was summarized on the BI tree topology and nodes were colored based on whether they were supported in BI, ML and/or MP analyses, respectively (Fig. 1). Molecular and morphological characters could be unambiguously optimized as synapomorphies on all major supported nodes (Tables 1-2).

The 'Northern Hemisphere clade' of Staphylinini (*sensu* Brunke *et al*,. 2016) was recovered in all analyses from strongly to weakly supported (PP = 0.85/1, BS = 0.85, JK=64). A single morphological and exclusive synapomorphy supports this node, the gular sutures slightly separated from each other (Fig. 3: 27, 0). The sister group of the 'Northern Hemisphere clade' could not be resolved with good support by any of the inference methods, though a 'Southern Hemisphere clade' (Figs. 1-3) was recovered by BI, ML and MP under IW but neither its monophyly nor the sister group relationship between *Afroquedius* and *Antimerus* within this group were supported. On the other hand, a less inclusive clade composed of *Afroquedius sexpunctatus*, *Antimerus punctipennis* and a monophyletic Amblyopinina, all mainly south temperate lineages, is present as sister group to the 'Northern Hemisphere clade' in the MP strict consensus topology under EW (Fig. 2). However, a clade composed of the Amblyopinina, Tanygnathinina and Hyptiomina appeared strongly to weakly supported by BI and ML (PP=0.87/1, BS=63), respectively, and five morphological (non-exclusive) synapomorphies (Table 1, Fig. 3). A sister group relationship between Tanygnathinina and Hyptiomina was strongly supported by all three methods (PP =0.91/1, BS = 0.90, JK=93) and six morphological (non-exclusive) synapomorphies (Table 1, Fig. 3).

Within the 'Northern Hemisphere clade', the current subtribes Cyrtoquediina, Erichsoniina, Indoquediina and Quediina were also recovered as monophyletic with strong support by all three methods (Figs. 1-2). Sister group relationships involving Indoquediina, Acylophorina and Erichsoniina were unresolved (Fig. 1). A clade composed of *Anaquedius vernix* and *Hemiquedius ferox* (Acylophorina) was strongly supported by BI and ML (PP=1, BS= 94) but weakly supported by MP (JK=64), and it was recovered with unsupported sister group relationships either to Erichsoniina by BI and ML or to (Indoquediina + (Quediina +Staphylinini propria)) clade by MP.

The monophyly of Quediina + Staphylinini propria was strongly to moderately supported by BI, ML and MP (PP=0.84/1, BS=73, JK=75) and one morphological non-exclusive synapomorphy (Table 1, Fig. 3: 20, 1). The monophyly of Staphylinini propria was strongly supported in all analyses (PP=0.84/1, BS=95, JK=99) and by three exclusive morphological synapomorphies (Table 1, Fig. 3). Here *Rientis* sp. was the sister group to the rest of Staphylinini propria (PP=0.83/0.99), within which the sister group relationship of Anisolinina to Staphylinina (PP=1), as well as the sister group relationship of Anisolinina + Staphylinina to the remaining main clade were well supported only by BI.

The monophyly of Anisolinina was strongly (PP=1) to moderately (BS=88, JK=76) supported by BI, ML and MP and a single morphological exclusive synapomorphy, prepectus of mesoventrite with acute ridge not connecting coxal cavities on posterior half (Fig. 3: 62, 1) in addition to three morphological non-exclusive synapomorphies (Table 1, Fig. 3). Staphylinina was recovered as a clade by all three methods, its monophyly strongly (PP = 1) to weakly supported (BS=67) by BI and ML but unsupported in the MP analyses under both EW and IW. Morphological characters supporting Staphylinina were all homoplastic (Table 1, Fig. 3). The Staphylinina clade was composed of two monophyletic and strongly supported subclades in all analyses (Figs. 1-2); one of the subclades included Eucibdelina (*Rhyncocheilus rugilipennis*).

The subclade of Staphylinini propria including representatives of *Algon*, *Barypalpus*, Philonthina and Xanthopygina appeared strongly to weakly supported by BI, ML and MP (PP=0.84/1, BS=54, JK=52). The clade *Barypalpus* + *Algon* was strongly supported by all three methods (PP=1, BS=100, JK=100) and three morphological (non-exclusive) synapomorphies (Table 1, Fig. 3). A sister group relationship of this clade to (Xanthopygina + *Philothalpus*) + Philonthina was recovered only by BI and MP under IW (K=6-42), but well supported only by BI (PP=0.84/1) and two morphological (non-exclusive) synapomorphies (Fig. 3). In ML and MP under EW analyses *Algon* + *Barypalpus* was recovered as sister group to either Xanthopygina+*Philothalpus* or only Xanthopygina in ML and MP, respectively, and without good support in either case.

The clade Xanthopygina + *Philothalpus* was recovered in the BI, ML and MP under IW topologies (K=6-48), being strongly to weakly supported by BI and ML (PP=0.99, BS=64) and not supported by morphological characters. In the MP under EW analysis *Philothalpus* was recovered as sister group to Philonthina, though without support. Xanthopygina was strongly supported by all three methods (PP=1, BS=100, JK=100) and three morphological exclusive synapomorphies: inferior marginal line of pronotal hypomeron continued as a separate entity beyond anterior pronotal angles and curving around them (46, 1) and abdominal terga 3 and 4 with curved ridge on disc (90, 1 and 91, 1). *Philothalpus* was recovered as a strongly supported group by all three methods (PP=1, BS=100, JK=100) and one single morphological exclusive synapomorphy, the sternopleural (anapleural) suture sinuate (Fig. 3: 56, 2) in addition to other non-exclusive synapomorphies (Table 2, Fig. 3).

Philonthina appeared as a strongly supported clade in all three analysis types (PP=0.84/1, BS=96, JK=100) and supported by several morphological non-exclusive synapomorphies (Table 1). The Philonthina clade is one of the backbone nodes for which BI showed differences in PP values depending on the inclusion of taxa lacking molecular data. If the five taxa with only morphological data are included

(i.e., with more than 95% missing data), Philonthina appeared as weakly supported by BI (PP=0.84), but still strongly supported by the other two methods. The first cladogenetic event within Philonthina separates the '*Hesperus* complex' from the remaining Philonthina. While the "*Hesperus* complex" appeared strongly supported by all types of analysis and one morphological (non-exclusive) synapomorphy (Table 2: only MP), the remaining philonthine clade is strongly to moderately supported only by BI and ML (PP=0.86/1, BS=84). This clade is also recovered as a monophylum in the MP topology, though without support. Two monophyletic groups strongly supported by all three methods are notable within the '*Hesperus* complex': the Australian clade (*Hesperus semirufus* + (*Hesperus haemorrhoidalis* + (*Actinus* sp. + *Leucitus* sp.))), and the New World clade (*Hesperus* sp. undescribed + (*H. apicialis* + *H. baltimorensis*)). The Philonthina clade sister to the '*Hesperus* complex' is divided into two subclades, both strongly supported by all three methods (Figs. 1-2). The first subclade (the '*Eccoptolonthus* clade') includes *Hesperus roepkei* + *H. laevigatus* in a strongly supported sister group relationship with *Eccoptolonthus* sp. This monophylum is strongly supported by all methods (PP=1, BS=100, JK=100) and one exclusive morphological synapomorphy (Fig. 3), as well as three non-exclusive synapomorphies (Table 1). The second subclade includes all the remaining representatives of Philonthina and is composed of two major monophyletic groups: one formed by *Cafius*- and *Philonthus*-complexes; and another formed by the clade (*Bisnius sordidus* + (*Gabrius*-complex + Neotropical lineage)).

The clade formed by *Cafius*- and *Philonthus*-complexes was strongly to weakly supported by BI, ML and MP (PP=0.92/1, BS=64, JK=76). While all three methods (PP=1, BS=96, JK=99) and some non-exclusive morphological synapomorphies (Table 2, Fig. 3) strongly support the '*Cafius* complex', its sister group is revealed differently by model-based methods and parsimony. In the BI and ML analyses, the "*Cafius* complex' is sister to a strongly to weakly supported '*Philonthus*-complex' composed of most sampled species of *Philonthus,* and*Gabronthus, Neobisnius*, *Rabigus* and *Taxiplagus*. In the MP tree under EW (Fig. 2), the '*Cafius* complex' appears sister to the '*Philonthus splendens* clade' formed by *Philonthus splendens* + (*Philonthus caeruleipennis* + *Philonthus nitidus*). The '*Philonthus splendens* clade' was strongly supported by all three methods (PP=1, BS=98, JK=90) and some morphological non-exclusive synapomorphies (Table 2). The monophyly of the '*Philonthus* complex' (including the '*Philonthus splendens* clade') is strongly to moderately supported by BI, ML and MP under IW (K=6-12) and one non-exclusive morphological synapomorphy by MP under IW (Table 2). The monophyly of the '*Philonthus* complex' was not supported by MP under EW.

The major philonthine clade formed by (*Bisnius sordidus* + (*Gabrius*-complex + Neotropical lineage)) was strongly to weakly supported by BI, ML and MP (PP=0.81/1, BS=85, JK=51). *Bisnius sordidus* is sister to the rest of the taxa in BI and ML analyses with weak support (PP=0.88, BS=54) (Figs. 1-2). This sister group relationship is also recovered weakly to unsupported by MP under IW (K=6), while the MP tree under EW showed an unresolved topology at this level. Nevertheless, all three methods have recovered two main clades, each strongly to weakly supported: 1) the "*Gabrius* clade" formed by all *Gabrius* and all *Bisnius* except *B. sordidus* (PP=0.96/1, BS=78, JK=78), and 2) the 'Neotropical lineage' formed by all Neotropical representatives of *Belonuchus* and the endemic Neotropical philonthine genera (PP=0.81/1, BS=66, JK=80). Both clades are supported only by non-exclusive morphological synapomorphies (Tables 1 and 2, Fig. 3). Within the '*Gabrius* complex', relationships are resolved and strongly to moderately supported in all analytical methods, though *Gabrius* was rendered paraphyletic by two *Bisnius* species.

Within the 'Neotropical lineage', two main subclades were recovered by BI, ML and MP under IW analyses. Only one of them was strongly to weakly supported by all three methods and included eight of the 12 Neotropical representatives of *Belonuchus* plus all *Paederomimus*, *Linoderus* and *Odontolinus*. Within this clade, *Belonuchus* sp. 5 appeared as sister to all other taxa which form a monophylum strongly to moderately supported by all three methods (PP=0.97/1, BS=87, JK=81) and two non-exclusive morphological synapomorphies (Table 1). This monophyletic group, here called '*Belonuchus* complex', consists of two clades. The first, the '*Belonuchus haemorrhoidalis* clade' (*Belonuchus rufipennis* + (*B. pollens* + (*B. rufipennis* group + *B. haemorrhoidalis*))) is strongly to moderately supported by BI, ML and MP (PP=0.95/1, BS=87, JK=79) and by one non-exclusive synapomorphy (14, 0: head without postmandibular ridge). The second clade, comprising three other species of *Belonuchus* plus some Neotropical endemic genera, is recovered and strongly supported by all three methods (PP=0.99, BS=99, JK=99) and by the single exclusive morphological synapomorphy, protibia with apical excavation (Fig. 3: 66, 1), and by several non-exclusive synapomorphies (Table 1). Although this second clade includes all *Paederomimus*, the genus was not recovered as monophyletic, with *P. nobilis* forming a strongly supported sister group with an undescribed species of *Linoderus* sp. and the remaining *Paederomimus* with *Belonuchus mimeticus* forming a group strongly to weakly supported by BI and ML (PP=0.91, BS=64) and one exclusive morphological synapomorphy, prosternum with transverse carina on

basisternum distinctly acute medially (Fig. 3: 40, 1). The other main subclade within the 'Neotropical lineage' was strongly supported only by the BI analysis with the 'DNA-only taxa' (PP=1), and it was not recovered by MP under EW. This subclade included a strongly supported - by all methods - *Chroaptomus* clade as sister group to a clade composed of all philonthine myrmecophiles (including *Quedius iheringi*) plus a few species of *Belonuchus* and *Philonthus*.

Molecular analyses

Analyses performed with only the molecular data yielded results that are overall similar (Fig. 4B) to those from the combined analyses (Tables 1 and 2, Fig. 1). The only difference that the molecular only results show are the following: 1) the 'Southern Hemisphere clade' was supported by BI (PP=0.81); 2) the 'Northern Hemisphere clade' was supported by both BI and ML but not by MP (PP=1; BS=78); 3) the monophyly of Anisolinina was supported only by BI (PP=0.92); 4) Staphylinina included *Rientis* sp. as sister group to the *Thinopinus pictus* + *Creophilus maxillosus* clade, though this relationship was supported only by BI (PP=0.99), while the monophyly of Staphylinina including *Rientis* sp. was unsupported; 5) the clade *Algon* + *Barypalpus* was supported by BI and MP as sister group to Xanthopygina (PP=1; JK=54), with *Philothalpus* supported as a sister group to Philonthina only by BI (PP=0.86); 6) within Philonthina, the '*Philonthus splendens* clade' appeared as a sister group to the '*Cafius* complex', but was supported by only BI (PP=0.83); 7) the clade composed of five of the six representatives of *Paederomimus* plus *Belonuchus mimeticus* was supported only by BI (PP=0.96).

Morphological analysis

An analysis of only morphological data recovered the monophyly of the following subtribes/lineages (Fig. 4A): Tanygnathinina, Hyptiomina, Cyrtoquediina, Erichsoniina, Indoquediina, Anisolinina, Xanthopygina and Philonthina and its Neotropical clade.

The position of *Holisus*

The position of *Holisus* (Hyptiomina) as sister group to Tanygnathinina, though supported by all three methods in both the combined and molecular analyses (Figs. 1-4), was further explored. The MP analysis using only morphological data (Fig. 4A) also recovered *Holisus* (Hyptiomina) as sister group to Tanygnathinina, but without support. To test for long branch attraction, the three representatives of Tanygnathinina were removed from the combined dataset (138 taxa) and a new MP analysis (135 taxa) was run under EW. The strict consensus of the 12 most parsimonious trees (MPTs) including JK support values is shown in the Supporting information. With Tanygnathinina removed, *Holisus* was recovered as an unsupported sister group to Amblyopinina, again far from Staphylinini propria and out of the 'Northern Hemisphere clade'.

Discussion

This study represents the first attempt to reconstruct the phylogeny of the mega-diverse tribe Staphylinini using both morphological and molecular data. We provide the first comprehensive phylogenetic hypotheses for its largest subtribe, Philonthina, and also for the 'Staphylinini propria', a core lineage of the tribe. Our results are largely congruent with the topologies of previous phylogenetic studies of the tribe, generally improving resolution for some lineages and removing inconsistencies. They confirm the backbone phylogeny of Staphylinini of Brunke *et al.* (2016) that was based on molecular data and included a post-analysis mapping of morphology. Thus, the simultaneous analysis of both sources of evidence reinforces the recently proposed subtribes Cyrtoquediina, Indoquediina, Acylophorina and Erichsoniina. Our results reject recent hypotheses (Solodovnikov and Schomann, 2009; Li and Zhou, 2011; Chani-Posse, 2013) of *Holisus* as a highly derived Philonthina and confirm its isolated taxonomic status as the sole member of subtribe Hyptiomina, finally eliminating controversies about its systematic placement (Newton, 1988). We propose the first robust phylogenetic hypothesis for Philonthina, which refines earlier results derived from regional, morphology-based analyses by Li and Zhou (2011) and Chani-Posse (2013). Our phylogenetic results indicate a path towards new, badly needed definitions of the polyphyletic mega-genera *Philonthus, Belonuchus* and *Hesperus*. The broad taxon sample surveyed to solve phylogenetic problems concerning Philonthina and *Holisus* was secondarily informative for inferring the first robust phylogeny of 'Staphylinini propria', with six major lineages. Four of these

lineages corroborated, to a major extent, the current subtribes Anisolinina, Philonthina, Staphylinina (including Eucibdelina) and Xanthopygina. Two additional clades involved taxa whose sister-group relationships and systematic position were considered a problem before and now form the basis for two newly erected subtribes: Algonina and Philothalpina. Here we discuss each of these major results in detail, moving from more basal to more terminal nodes (or lineages).

1. Hyptiomina and the 'Southern Hemisphere clade' of Staphylinini

Newton (1988) was the first to recognize *Holisus* as a member of the tribe Staphylinini. Since then it remained in the monogeneric subtribe Hyptiomina, with unclear sister-group relationships. Newton and Thayer (1992) summarized the nomenclatural history of this family-group name. Recent controversy about the affinities of *Holisus* (for details see Introduction) brought conflicting evolutionary and biogeographic scenarios for the origin of Hyptiomina, and the systematic status of this subtribe. A sister-group relationship between Hyptiomina and Tanygnathinina was first supported in a morphological analysis of the subfamily Staphylininae based on adult and larval characters (Solodovnikov and Newton, 2005) and later in the first molecular-based analysis of the tribe Staphylinini (Chatzimanolis *et al.*, 2010), though both these studies had rather limited taxon sampling. On the other hand, *Holisus* was consistently nested inside Philonthina in all later morphological analyses based on larger taxon sample and only adult characters (Solodovnikov and Schomann, 2009; Li and Zhou, 2011; Chani-Posse, 2013). A relationship between *Holisus* and *Atanygnathus,* the latter genus of Gondwanan origin (Chatzimanolis *et al.*, 2010; Solodovnikov, 2012), offered a biogeographically plausible interpretation of the disjunct distribution of the former. Within this phylogenetic framework, the distribution of *Holisus* in the Neotropics (the great majority of species) and in West Africa (one species and two undescribed species, for details see Taxonomy section) would be consistent with ancient connections between South America and Africa. This seemed unlikely, however, given the strong morphological and ecological differences between these highly derived genera. Characters that supported their relationship in Solodovnikov and Newton (2005) were largely morphological reductions. On the other hand, the occurrence of *Holisus* in West Africa was inconsistent with a rather terminal position within the Neotropical Philonthina. Given that Philonthina is presumably a relatively young lineage of Staphylinini that had not even appeared by the Early Cretaceous (Solodovnikov *et al.*, 2013), a deeply nested *Holisus* within Philonthina would imply a remarkable case of trans-Atlantic dispersal between the Neotropics and Africa, as the land connection between South America and Africa ceased during the Albian (Friis *et al.*, 2011). Given this and the fact that both *Holisus* and *Atanygnathus* are always recovered on long branches, the negative effect of long branch attraction (LBA) was a reasonable suspicion (Chatzimanolis *et al.*, 2010; Chani-Posse, 2013).

Our analysis, where all preventive measures against LBA have been taken into account, corroborates the hypothesis that Hyptiomina is the sister group to Tanygnathinina. Among the morphological characters supporting this grouping in the analysis, three are highly homoplastic (basisternum without pair of macrosetae, protarsi with tarsomeres 1-4 more or less cylindrical, not transversely widened, not flattened dorso-ventrally and without pale adhesive setae), while the three remaining characters seldom occur out of Tanygnathinina and Hyptiomina: antennae inserted at the anterior margin of frontoclypeus, elytron without subbasal ridge and hind wing without vein MP3. The antennal insertion and the hind wing venation character states are also shared with the myrmecophilous genera of Philonthina. These two characters as well as others with states shared between Hyptiomina and Philonthina (see Supporting information) have contributed in the past to the hypothesis of *Holisus* being nested within Philonthina. Unlike members of Philonthina and all 'Staphylinini propria', *Holisus* lacks the posterior scutellar ridge on the scutellum, a diagnostic character state of the Tanygnathinina and Amblyopinina (Solodovnikov, 2012). Also, an examination of the aedeagus of various species of *Holisus* (not coded in the matrix here) revealed intermediate stages between the aedeagal type characteristic of Amblyopinina and Tanygnathinina, and the highly simplified form, typical of *Holisus*. Within the context of our present phylogeny, *Holisus* remains in its own subtribe, within a lineage of Staphylinini whose origin and early diversification is associated with Gondwana. Presumably, Hyptiomina and Tanygnathinina are highly derived branches of that Gondwanan lineage which strongly diverged from their common ancestor towards very different specialisations, and whose more generalised stem lineages went extinct. By analogy with the 'Northern Hemisphere clade' of Staphylinini introduced in Brunke *et al.* (2016), here we call its sister Gondwana-derived lineage the 'Southern Hemisphere clade'. While Hyptiomina is a very peculiar and relatively small group within this clade, the bulk of the Southern Hemisphere clade is formed by hundreds of species in the subtribe Amblyopinina that dominate the south temperate Staphylinini fauna in the south temperate areas of the globe.

2. Phylogeny of Philonthina, especially of its 'Neotropical lineage'

The monophyly of Philonthina was strongly supported here by all three methods. Morphological characters supporting the subtribe were, though homoplastic, highly diagnostic for nearly all philonthines. The lack of a hypostomal cavity, seta alpha on the mentum and empodial setae, and the presence of a posterior basal transverse carina on abdominal tergum 3, although plesiomorphic, are character states unique for Philonthina among Staphylinini propria. The superior marginal line of the pronotal hypomeron distinctly deflected under the anterior angles and an absence of empodial setae are also observed in Erichsoniina and Hyptiomina (the first character also in Staphylinina andAnisolinina). Finally, the abdominal prototergal glands formed as invaginated capsules with smaller openings is a state only observed outside of Philonthina in *Quedius antipodum*, *Xanthopygus xanthopygus* and *Strouhalium gracilicorne* (Brunke and Solodovnikov, 2013). The combination of the deflexed superior line of pronotal hypomeron and the lack of empodial setae was previously considered to be diagnostic of Philonthina by Smetana and Davies (2000) and Chani-Posse (2014a). Further characters that have been used traditionally by the above authors and others to recognize philonthines, were shown by our analyses to be highly homoplastic (ligula entire to slightly notched, disc of neck impunctate, postcoxal process absent) or common throughout Staphylinini propria (infraorbital ridge reaching postgenal ridge or slightly extending beyond postgenal ridge, dorsal basal ridge present, notosternal suture absent). Within Philonthina, the 'Neotropical lineage' was consistently recovered here as monophyletic as well as its main component, the so-called '*Belonuchus* complex', in agreement with a previous, more limited morphological study (Chani-Posse, 2013).

Belonuchus, as currently treated (Li and Zhou, 2011) is represented by two lineages: the 'true *Belonuchus*', including the type species (*B. haemorrhoidalis*) and 186 other New World species; and a lineage formed by Old World species originally placed in *Trapeziderus* Motschulsky, a genus currently in synonymy with *Belonuchus*. In our study, the Old World lineage was represented by *Belonuchus imitator*, which belongs to the same lineage as *B. bicolor* (Motschulsky), the type species of the genus *Trapeziderus* (Li and Zhou, 2011). While the Old World lineage is clearly a part of the *Hesperus* complex, the 'true *Belonuchus*' are phylogenetically remote from the former and part of the Neotropical clade. Therefore, *Trapeziderus* should be reinstated as a genus to contain the 'Old World *Belonuchus*', while the genus *Belonuchus* must be redefined. After our study, two morphological characters support the '*Belonuchus* complex': the maxillary palpus with palpomere 4 subcylindrical, also present in the *Hesperus* complex, *Eccoptolonthus*, *Holisus* and some Amblyopinina; and the basisternum of prosternum transversely carinate, which otherwise only occurs in other four species out of this complex within the 'Neotropical lineage' (see Supporting information). The '*Belonuchus* complex' consisted of two clades, one of which included the type species of the genus and is supported by the absence of the postmandibular ridge. This character state, though homoplastic, was constant within what we call the '*Belonuchus haemorrhoidalis* clade'. The second clade included other species of *Belonuchus* plus several Neotropical endemic philonthine genera and is characterized by the protibiae with an apical excavation, an exclusive synapomorphy. *Paederomimus*, the most speciose of the endemic Neotropical philonthine genera, was not recovered as monophyletic, though all representatives were recovered inside this second clade. Still, six of the seven representatives (together with *Belonuchus mimeticus*) were recovered in a well-supported group, characterized by one exclusive synapomorphy: basisternum of prosternum with transverse carina distinctly acute medially. Since the type species of the genus, *P. difformiceps* Sharp, does not share this condition (Chani-Posse, pers. obs.) and was not included in our taxon sample, we can not introduce a new concept for *Paederomimus*. We also refrain from proposing a *Paederomimus sensu lato* concept that would include *Linoderus*, *Odontolinus* and *Pescolinus* (not included here) as these genera are distinct enough to be kept as such (Chani-Posse, 2014ab). Given the internal relationships of the *Belonuchus* complex revealed in our study, we propose to restrict the definition of *Belonuchus* to that of the '*Belonuchus haemorrhoidalis* clade' (see Systematics).

3. Phylogeny-based limits for large, currently artificial genera

The most speciose genera of Philonthina are *Philonthus* Stephens (1350 spp.), *Gabrius* Stephens (ca. 400 spp.), *Hesperus* Fauvel (over 220 spp.), *Belonuchus* (over 200 spp.), *Bisnius* Stephens (83 spp.) *Neobisnius* Ganglbauer (72 spp.), *Gabronthus* Tottenham (ca. 50 spp.), *Paederomimus* (58 spp.) and *Cafius* Stephens (over 40 spp.) (Newton, unpublished database). Except *Neobisnius*, the monophyly of *Philonthus, Gabrius*, *Bisnius*, *Gabronthus* (Smetana, 1995; Solodovnikov and Schomann, 2009; Chani-Posse, 2013), *Belonuchus, Hesperus* (Schillhammer, 2002, 2016; Li and Zhou, 2011; Chani-Posse, 2014a), *Cafius* (Jeon *et al.*, 2012), and *Paederomimus* (Chani-Posse, 2014a) has been questioned. Current diagnoses for those genera are based on a combination of plesiomorphies for Philonthina involving the structure of front tarsi (sexually dimorphic or not), pronotum (superior marginal line distinctly deflected

or not, position of the lateral puncture relative to the superior marginal line), last segment of maxillary and labial palpi (shape and length), mesoventrite (transversely carinate or not, shape of apical portion), hind tarsi (relative length of tarsomeres 1 and 5) and sternum 9 (basal portion symmetric or asymmetric). In addition to the plesiomorphic nature of these characters, some of them may show continuous variation among taxa or are sexually dimorphic.

Our results confirm the non-monophyly of *Philonthus*, *Bisnius*, *Gabrius*, *Hesperus*, *Cafius*, *Belonuchus* and *Paederomimus*. While we acknowledge that generic limits for these taxa are difficult to settle in one step due to the number of species and amount of alpha-taxonomic work involved, we propose that further revisionary work should consider the narrower generic concepts proposed herein.

Philonthus and allied genera. The cosmopolitan genus *Philonthus* is the fourth largest genus within Staphylinidae and the largest within Staphylininae (Newton, pers. comm.). The study of its species has continued mostly based on Smetana´s generic diagnosis (e.g., Smetana, 1995, Schillhammer, 1998,1999a, 2000, 2001a, 2003, Chani-Posse, 2010, Hromádka 2008ab, 2009, 2010abc). Our model-based, combined analyses showed a "*Philonthus* complex" within which *Gabronthus*, *Neobisnius*, *Rabigus* and *Taxiplagus* were nested, while two other *Philonthus* species were recovered far from this complex in the Neotropical lineage of Philonthina. Only one morphological and highly homoplastic character supports the "*Philonthus* complex": the gular sutures not joined before neck, extended close to each other at the base of the head capsule. The "*Philonthus splendens* clade", which includes the type species of the genus, was supported by two morphological characters, one of which is highly homoplastic (head with postmandibular ridge separate from mandibular base) and the other (prepectus of mesoventrite with ridge connecting coxal cavities on posterior half distinctly arcuate to obtuse) has also been observed in some *Gabrius* and it is common in the Neotropical lineage of Philonthina. On the other hand, the "*Philonthus* complex" was not recovered here by the molecular-based analyses showing the "*Philonthus splendens* clade" as sister to the "*Cafius* complex", in agreement with the parsimony-based combined analysis under equal weights. Our results show that the current concept of *Philonthus* (Smetana, 1995), even if restricted to its Holarctic species, is clearly polyphyletic with respect to at least four other genera. It is likely that the genus *Philonthus* should be restricted to the "*Philonthus splendens* clade" and that the generic assignment of many of its species should be revised.

The genera *Bisnius* and *Gabrius* were not closely related to any of the *Philonthus* representatives in our study. *Bisnius sordidus*, a cosmopolitan species belonging to the same species-group as the type species of the genus, *B. cephalotes* (Gravenhorst) (Smetana, 1995: *cepahlotes*-group), was recovered as the sister group to a major clade consisting of some representatives of *Bisnius, Gabrius,* and the Neotropical lineage. The remaining *Bisnius* and *Gabrius* appeared together in a natural group supported by two morphological characters, one highly homoplastic (first metatarsomere shorter than fifth or at most both tarsomeres subequal), and the other (male sternum 9 with basal portion more or less symmetrical) plesiomorphic as it also occurs in *Arrowinus*. Both character states seem to occur in only a few genera within Staphylinini (see also Brunke and Solodovnikov, 2013). Each of the extra-Neotropical species of *Gabrius* in our analyses corresponds to a different species-group (Smetana, 1995, Schillhammer, 1992, 1997). The *nigritulus*-group, where the type species of the genus is included, is here represented by *G. picipennis* (Smetana, 1995). Together with two Neotropical species as its sister group, *Gabrius picipennis* was sister to the Palaearctic *G. keysianus* (Schillhammer, 1992: *keysianus*-group) plus the Oriental *G. trossuloides* (Schillhammer, 2001c: *submetallicus*-group), together forming a well-supported clade. One of the morphological characters supporting this clade (male sternum 9 not distinctly emarginate on its distal portion) has been cited by Schillhammer (1997) as diagnostic for the *nigritulus*-group. The other subclade was entirely composed of Nearctic taxa and included *Gabrius ovaliceps*, *G. brevipennis*, as well as *Bisnius blandus* and *B. picicornis*, but without support from morphological characters. Without enough evidence for the phylogenetic status of *Bisnius*, we refrain from changes to its current concept (Smetana, 1995).

Hesperus. Most *Hesperus* are distributed in tropical areas of the Oriental and Pacific regions including New Guinea (Newton, unpublished database). Although Smetana (1995) found that the six Nearctic species of *Hesperus* formed a natural group, he recognized that characters defining this group "may pose difficulties for specimens from tropical areas, particularly from New Guinea, due to certain variability and/or absence of some character states". Schillhammer (2002) also noticed that characters defining *Hesperus* were not enough to clearly define the genus and considered it to be "a polyphyletic assemblage" (Schillhammer, 2016). Still, he decided to maintain that concept until a revision covering at least the Palaearctic and Oriental regions is achieved. Non-monophyly of *Hesperus* was confirmed in a formal phylogenetic analysis by Li and Zhou (2011). Our results here also corroborate those previous hypotheses, as *Belonuchus imitator* and the genera *Actinus*, *Hesperopalpus*, *Hybridolinus* and *Leucitus*

were nested within the "*Hesperus* complex". On the other hand, the "*Hesperus* complex" was itself strongly supported, and shared one homoplastic morphological character state (the mesocoxae not distinctly recessed, positioned on approximately the same plane as intercoxal process and metaventrite) which is a common condition in the Neotropical lineage of Philonthina and some Staphylinina. Noticeably, *H. borneensis* was recovered by all three methods in the most remote position relative to other representatives of its genus. Two strongly supported and biogeographically meaningful subclades were recognized within the "*Hesperus* complex": the Australian subclade (including *Actinus* and *Leucitus*), and the New World subclade. The New World subclade corresponds to Smetana´s concept of *Hesperus*, which includes the type species of the genus, *H. rufipennis* (Gravenhorst) and other Palaearctic and Nearctic species (Smetana, 1995, Schillhammer *et al.*, 2007).

Cafius-complex. Jeon *et al.* (2012) have recently proposed to integrate the genus *Cafius* and allied genera *Phucobius*, *Remus* and *Thinocafius* into a new system of species-groups, based on their molecular phylogeny, which showed *Cafius* to be paraphyletic with respect to the other genera. As they did not explore morphological characters, the authors refrained from changes to the generic classification of these taxa. Our results agree with those of Jeon *et al.* (2012) concerning the monophyly of the *Cafius*-complex (*Phucobius* not included in the current analysis). Our "*Cafius*-complex" was well supported by both molecular and morphological data. Based on this evidence, we propose to define the so called *Cafius* complex as a natural unit here (see Systematics), but we refrain from taxonomic changes in the present study given the restrictions imposed by our current taxon sampling.

4. Staphylinini propria

Monophyly and sister group. Staphylinini propria is further corroborated here as a natural group with the same morphological characters supporting its monophyly that were previously known as part of its diagnosis (Brunke *et al.*, 2016). Also, we confirm its sister group relationship to Quediina and previous hypothesis about its Quediina-like ancestor (Brunke *et al.*, 2016). Exclusive synapomorphies of 'Staphylinini propria' here are: head with dorsal basal ridge and hypostomal cavity, as well as transversely carinate metacoxae. Four other non-exclusive synapomorphies are: head with postmandibular sulcus, pronotum and prosternum at least partially fused (i.e., pronotosternal suture missing in part of cavity) and elytron without humeral spines or spine-like setae. Presumably, many of these morphological features are related to changes in locomotion from moving within substrates such as leaf litter, as many Quediina do, to predominately running on the surface. Other features may be related to changes in modes of prey capture or prey choice affecting head mobility and mandibular strength. The evolution of a dorsal basal ridge in Staphylinini propria (as far as known present in all taxa except highly modified *Euristus* Fauvel and *Descarpentriesiellus* Jarrige) and transverse carina on the metacoxae (secondarily lost in very few genera) may indicate a strengthening of both the base of the neck and coxae. Within Staphylinini propria, all taxa with a postmandibular sulcus either do not have an infraorbital ridge or, if one is present, then it is never in its plesiomorphic, i.e. complete condition. Congruently, all taxa outside of Staphylinini propria with a complete infraorbital ridge do not have a postmandibular sulcus. This correlation may suggest that a reduction of the infraorbital ridge is associated with the development of a postmandibular sulcus, as was already addressed in a previous study (Chani-Posse, 2014a). A possible trend can be observed from a complete infraorbital ridge in the plesiomorphy-rich groups like Quediina and Acylophorina to reduction in Staphylinini propria, where it is often completely lost. Presumably, morphological innovations have enabled the ancestors of Staphylinini propria to expand into a wider range of environments and diversify into different lineages.

Rientis and *Barypalpus.* Smetana (1977) removed *Rientis* from Quediina and placed it in the subtribe Xanthopygina. Later, Schillhammer (1999b) placed *Barypalpus* in synonymy with *Rientis*. *Rientis* became *incertae sedis* within Staphylinini after Chatzimanolis (2014) removed it from Xanthopygina in an effort to restrict the subtribe to a monophyletic core of Neotropical taxa. Our results support the placement of *Rientis* outside Xanthopygina but contradict its synonymy with *Barypalpus*. Here *Rientis* was recovered by all three inference methods as the sister group to all other Staphylinini propria in the combined analyses, while *Barypalpus* formed a lineage with the genus *Algon*. However, our analysis of only molecular data showed *Rientis* as part of an unsupported clade within Staphylinina. We propose that *Barypalpus* is removed from synonymy with *Rientis* and that the latter is redefined. Even though our results suggest that *Rientis* is a phylogenetically isolated taxon deserving its own subtribe and whose similarities to other Staphylinini propria are plesiomorphic, its phylogenetic placement was not conclusive. Thus, it remains Staphylinini *incertae sedis*.

Anisolinina. The subtribe Anisolinina Hayashi, 1993 was originally defined based on differences in character states of the pronotum, prosternum and the mesoventrite shown by the genera *Anisolinus* Sharp, *Amichrotus* Sharp, *Hesperosoma* Scheerpeltz and *Tympanophorus* Nordmann versus those of *Philonthus* (Philonthina), *Xanthopygus* Kraatz (Xanthopygina), *Creophilus* Leach, *Hadropinus* Sharp and *Liusus* Sharp (Staphylinina). The concept of Anisolinina was later broadened by Smetana and Davies (2000). Both Hayashi (1993) and Smetana and Davies (2000) recognized a resemblance between members of this subtribe and those of the *Philonthus cyanipennis* group in general habitus and in the development of the mouthparts. Within our morphological dataset, Anisolinina and *Philonthus caeruleipennis* (a species from *Ph. cyanipennis*-group) shared only one character: the abdominal prototergal glands showing a well-developed acetabulum. Since this character occurs only once within our sample of Philonthina (*P. caeruleipennis*) but is commonly found in other subtribes, also outside of Staphylinini propria, we conclude that this condition is a reversal to the plesiomorphic character state for *P. caeruleipennis*. Later, Schillhammer (2004b) recognized two distinct lineages within Anisolinina, the *Anisolinus* lineage and the *Tympanophorus* lineage, mainly based on shape and development differences in the "elevated ridge of mesoventrite". Herein the subtribe Anisolinina was supported by characters already recognized in previous studies, including the unique synapomorphy: prepectus of mesoventrite with an acute ridge not connecting coxal cavities on posterior half, which is here considered homologous to the "elevated ridge of mesoventrite" of Schillhammer (2004b). Staphylinina has been previously resolved as the sister group to Anisolinina by Chatzimanolis (2014) and Brunke *et al.* (2016). In the present study we have found support for this sister-group relationship but from only the BI combined analysis and no morphological characters were found to support this node.

Staphylinina and Eucibdelina. Smetana and Davies (2000) provided the most recent concept of Staphylinina and its monophyly has not been challenged since then (Solodovnikov and Schomann, 2009; Chatzimanolis *et al.*, 2010; Brunke and Solodovnikov, 2013; Brunke *et al.*, 2016). However, this definition stems from pre-cladistic and Holarctic fauna-based classifications of the tribe Staphylinini, becoming more inclusive when more genera were added later but still vaguely defined by two character states: a bilobed or notched ligula and the superior marginal line of pronotal hypomeron deflected under anterior angles of the pronotum (Solodovnikov and Brunke, 2016). In the present study, Staphylinina is defined by a combination of plesiomorphies including the labium with a more or less bilobed ligula. The presence of a distinctly emarginate to bilobed ligula has been reported for all members of this subtribe with the exception of some species of *Dinothenarus* (Smetana and Davies, 2000). Outside of Staphylinina, we observed this state in *Pammegus* (Anisolinina), *Xanthopygus* (Xanthopygina) and *Rientis.* Solodovnikov and Brunke (2016) summarized internal relationships within Staphylinina, where two groups of genera had been defined so far: the '*Creophilus*-complex' of Clarke (2011), and the '*Eucibdelus* lineage' of Schillhammer (2001b) (=Eucibdelina). The '*Staphylinus*-complex' was more loosely defined by Smetana and Davies (2000), who included the genus *Creophilus* among its members. Both Chatzimanolis *et al.* (2010) and Brunke *et al.* (2016) recovered the '*Creophilus*-complex'as a sister group to the '*Staphylinus*-complex' of Smetana and Davies (2000). The same lineages were recovered by all three methods in our study, but with a novel result: Eucibdelina was nested within the '*Staphylinus*-complex'. The inclusion of Eucibdelina in Staphylinina confirmed previous hypotheses about its close relationship to the latter by Hayashi (2005) but eliminated the necessity of the separate subtribe for this lineage. Although only one representative of Eucibdelina was available to us for DNA studies (*Rhyncocheilus rugulipennis*), which does not belong to the type genus of Eucibdelina (*Eucibdelus* Kraatz), it adequately represents the '*Eucibdelus*-lineage' according to Schillhammer (2004a) and Hayashi (2005). We propose that the subtribe Eucibdelina, currently treated as valid (Bouchard *et al.*, 2011), is synonymized with Staphylinina.

Algon and *Barypalpus.* The phylogenetic position of *Algon* has been a long standing problem. Smetana (1977) removed *Algon* from Quediina and placed it in the subtribe Xanthopygina. Since then, the placement of *Algon* within Xanthopygina has been questioned (Solodovnikov, 2006; Solodovnikov and Schomann, 2009; Schillhammer, 2006; Chatzimanolis *et al.*, 2010) so that *Algon* was finally considered as Staphylinini *incertae sedis* by Chatzimanolis (2014). Here we found that *Algon* forms a strongly supported lineage with the genus *Barypalpus*, which we reinstate from synonymy with the genus *Rientis* (see above discussion about *Rientis* for more details). The sister group relationship of *Barypalpus* + *Algon* to a large clade including (Xanthopygina+*Philothalpus* + Philonthina) was supported by BI and two non-exclusive synapomorphies on our combined analysis. One of them, metatarsomeres 3-5 with dorsal surface glabrous along midline and chaetotaxy developed only at margins, though homoplastic, has only

been otherwise observed in Acylophorina and the *Quedionuchus* lineage (Brunke and Solodovnikov, 2013). *Philothalpus* shows an apparent reversal to the plesiomorphic state with setose metatarsomeres but a few species do have the opposite state (*P. porphyros* and *P. rugosus*). Alternative sister groups of *Algon* + *Barypalpus* were recovered by ML (Xanthopygina + *Philothalpus*), and by MP under EW and our molecular only analyses (Xanthopygina), but both these topologies were unsupported. In the latter case, *Philothalpus* was the sister group to Philonthina. Given the contradictory hypotheses among inference methods and datasets, we cannot be conclusive here about the relationships among the clades *Barypalpus* + *Algon*, Xanthopygina, *Philothalpus* and Philonthina. What became evident, though, is that both *Barypalpus* + *Algon* and *Philothalpus,* are two isolated lineages that would remain as such, regardless of their sister group relationships. Both *Algon* and *Barypalpus* occur in the East Palearctic and Oriental regions (Schillhammer, pers. obs.) and their sister group relationship is a novel result of our study. The earlier affiliation of *Algon* with Xanthopygina was due to the front angles of pronotum "meeting the prosternum in the typical staphylinine way" and "the mandibular ridge and groove and the shifting of the eyes dorsally" (Smetana, 1977). The so-called "groove" was interpreted by Smetana (1977) as non-homologous to the infraorbital ridge of quediines - to which *Algon* was firstly assigned by Sharp (1874) – but commonly occurring in Xanthopygina. This "groove" in *Algon* was later interpreted as a "postmandibular sulcus" by Schillhammer (2006). The "postmandibular sulcus" is used here in the sense of Schillhammer (2006: Figs. 70-71), its presence typical among members of Staphylinini propria, though much less extended anteriad in most Philonthina. *Algon* currently contains 70 species (Schillhammer, 2006, 2008, 2011; Hayashi, 2011; Assing, 2015), while its sister group *Barypalpus* is known from four species (*B. ruficornis*, one undescribed species from Laos and other two undescribed species from China). We propose to erect the new subtribe Algonina for the clade *Algon*+*Barypalpus*.

<u>*Xanthopygina and Philothalpus.*</u> The subtribe Xanthopygina is currently a group of 30 genera distributed in the New World tropics. The limits of the subtribe were recently settled by Chatzimanolis (2014) based on a molecular-based phylogeny that resolved Xanthopygina as monophyletic with the exception of the Neotropical genus *Philothalpus* traditionally placed within Xanthopygina (e.g., Chatzimanolis and Ashe, 2005, Asenjo and Ribeiro Costa, 2009). After Chatzimanolis (2014) recovered *Philothalpus* as the sister taxon to all other 'Staphylinini propria' sampled in his study, the genus has been considered *incertae sedis* in the tribe Staphylinini. In the present study, *Philothalpus* was recovered as a distinct, monophyletic lineage within 'Staphylinini propria' by combined and partitioned analyses using all three methods. A sister group relationship to Xanthopygina was resolved by BI and ML combined analyses but no morphological characters supported this grouping. Xanthopygina was recovered with strong support by all three methods in addition to three morphological synapomorphies, including the inferior marginal line of the pronotal hypomeron continued as a separate entity beyond anterior pronotal angles and curving around them. This character state is shared by the great majority of xanthopygines and does not occur in *Philothalpus*. Chatzimanolis (2014) rather focused on the superior line of the pronotal hypomeron than on the inferior line in his diagnosis for the subtribe. According to Chatzimanolis, members of Xanthopygina can be typically identified by the superior line of the pronotal hypomeron, which continues to the anterior edge of the pronotum without deflection and is completely visible from above, the presence of a long postmandibular ridge on the head, and the elongate urogomphi present in the known larvae. The superior marginal line of pronotal hypomeron not distinctly deflected under anterior angles was shown here to be a homoplastic character across Staphylinini. Within Staphylinini propria, this condition was observed in *Rientis*, *Algon* + *Barypalpus*, Xanthopygina, *Philothalpus* and three myrmecophile genera within Philonthina. Among the several synapomorphies defining *Philothalpus* here, only one appears as exclusive: the sinuate sternopleural (anapleural) suture. However, this character state also occurs in the unrelated philonthine *Flohria* (Sharp) (Chani-Posse, 2014a; Chani-Posse and Newton, 2015), a genus not included in our analysis. Although sister group relationships of *Philothalpus* remain somewhat unclear, our study supports the creation of a new subtribe for this genus.

5. Basal relationships of Staphylinini

Our analysis recovered two main clades within Staphylinini: the well supported 'Northern Hemisphere clade' earlier defined in Brunke *et al.* (2016), and a 'Southern Hemisphere clade' supported only by BI of our molecular only dataset. Within this southern clade, *Holisus* (Hyptiomina) was resolved as the sister group to Tanygnathinina, both these subtribes formed the sister group to Amblyopinina, and these four taxa together formed the sister group to *Afroquedius+Antimerus*. As already discussed, the close relationship between *Holisus* and Tanygnathinina, corroborated in our study, is not an artifact. For basal relationships outside 'Staphylinini propria' the only incongruence between our results and Brunke *et al.* (2015) concerned unsupported nodes. Such is the case of South African *Afroquedius*, which was

recovered here together with Australian *Antimerus*. Although both taxa remain as Staphylinini *incertae sedis*, a sister group relationship of *Afroquedius* to Amblyopinina was hypothesized by Solodovnikov and Schomann (2009) and recently corroborated by Brunke *et al.* (2016). The latter hypothesis is morphologically plausible as both taxa share an aedeagus with a paramere closely affixed to the base of the median lobe. In our study, this character state was found to be a homoplastic apomorphy supporting Amblyopinina + (Tanygnathinina + Hyptiomina). Overall, morphological characters proposed by Brunke *et al.* (2016) for the diagnosis of each of the subtribes supported the corresponding nodes in our study. The potential sister group relationship of *Antimerus* and *Afroquedius* was here supported by only two highly homoplastic morphological characters.

By analogy to the 'Northern Hemisphere clade' that is notably depauperate on isolated Gondwana-derived island continents like Australia or New Zealand, we propose the informal name 'Southern Hemisphere clade' for its sister group since it is dominated by the diverse and numerous species of Amblyopinina, the most prevalent subtribe in the south temperate zone. *Antimerus* and *Afroquedius* are also restricted to the Southern Hemisphere, while *Holisus* is disjunct between the Neotropics and Afrotropics. The globally distributed *Atanygnathus* may have originated in South Africa where its putative sister group, *Natalignathus*, occurs (Solodovnikov, 2005). Presumably, such a clear biogeographic signal in the basal divergences of Staphylinini results from the long isolated evolution of its early lineages on Laurasia and Gondwana after the break up of Pangaea in the Late Jurassic (Cecca *et al.*, 1993). Although this scenario has recently found some additional evidence from the taxonomic composition and age of the Early Cretaceous Staphylinini and allied fossils of the Chinese Yixian Formation (Solodovnikov *et al.*, 2013), its rigorous exploration needs more data and analyses.

6. Character-based evidence from molecular and morphological data

Molecular and morphological synapomorphies were identified for all supported major nodes that correspond to higher and lower levels of the systematic classification of Staphylinini. This indicates that character-based phylogenetic evidence indeed exists within our combined dataset for each of these lineages (Simmons and Randle, 2014), even if their respective clades were not recovered or supported by MP under EW and/or IW. Topologies from the three inference methods were very similar to each other, with most major lineages and clades being supported by all three methods and common apomorphic characters. Most phylogenetic signal was found to be concentrated in the genes *TP, CAD*, *COI* and ArgK, consistent with other reports of their utility for resolving evolutionary relationships in beetles (Wild and Maddison, 2008, Chatzimanolis, 2014). *TP* was the main contributor in our analysis for the recovery of relationships at or above the subtribe level (Table 1) while *COI* succeeded in recovering relationships below the subtribal level (Table 2). However, *CAD* accounted for the greatest number of synapomorphies at both higher and lower hierarchical levels, which is in agreement with previous findings on beetle phylogenies (e.g., Maddison, 2012; Robertson *et al.*, 2013; Bukontaite *et al.* 2014; Chatzimanolis, 2014; Brunke *et al.*, 2016). It should also be kept on mind that our taxon sample was not as complete for *TP* and *CAD* compared to the other four genes, with 101 taxa for *TP*, 85 for *CAD* A and 70 for *CAD* C. On the other hand, the genes contributing the fewest synapomorphies were 28s (Tables 1, 2) and *Wg* (Table 1).The poor performance of *Wg* at or above the subtribal level in our study differs from that observed in Brunke *et al.* (2016). Since this gene was the most complete for our taxon sample (133 sequences), this discrepancy is perhaps due to the limited number of basal Staphylinini in our study. Twenty-six morphological characters provided exclusive synapomorphies from both ML and MP analyses, here shown on our ML topology (Fig. 3). Most of them were distributed among the head, including mouthparts (8), prothorax (5), mesothorax, including elytra (5) and legs (5), while the abdomen and structures associated with genitalia contributed two characters each. Overall, model-based analyses provided more resolution of both basal and terminal nodes than the phylogeny inferred by MP under EW. Nonetheless, a comparable amount of resolved nodes were obtained by MP under IW within a broad range of K values (K=6-36), most of them in agreement with those obtained from the model-based analyses in terms of node support and synapomorphies. Although the highest number of synapomorphies was found by ML, exclusive synapomorphies were always recovered by MP under EW and/or IW.

When the analyses were partitioned (molecular vs. morphology data), the morphology-based phylogeny provided resolution only at the subtribal level, leaving both backbone and terminal nodes mostly unresolved. This is in contrast with the resolution shown by the molecular-based phylogeny, which is highly congruent with that shown by the combined data.

Conclusions and future directions

The phylogeny inferred in the current study contributes to a comprehensive understanding of evolutionary relationships within the tribe Staphylinini, following and complementing previous studies. It brings us closer to the natural classification of this distinct tribe of rove beetles. After Brunke *et al.* (2016) improved the higher classification of Staphylinini, internal relationships within the megadiverse 'Staphylinini propria' clade remained unclear. Here, the monophyly of 'Staphylinini propria' was supported as well as that of each of its currently known subtribes Anisolinina, Staphylinina, Xanthopygina and Philonthina. Sister group relationships among these subtribes and those of some puzzling, hitherto unassigned genera are now clarified. Two new subtribes, Algonina and Philothalpina, are erected while Eucibdelina is synonymized with Staphylinina. The genus *Holisus* was found to be an independent lineage of the 'Southern Hemisphere clade' of Staphylinini, and we reject an earlier hypothesis of it being a highly derived subcortical genus of Philonthina. Our results confirm the status of Hyptiomina as a separate, monogeneric subtribe and suggest that its disjunct distribution is the result of ancient vicariance between South America and Africa at the end of Early Cretaceous. A rigorous test of this scenario would involve phylogenetic dating of our phylogeny using a fossil-calibrated molecular clock.

Morphological characters traditionally used in the classification of Staphylinini, both at subtribal and generic levels, were demonstrated to be of limited value. Pronotal morphology and head ridges were historically important in higher-level classification across Staphylinini, while morphology of the front tarsi and mouthparts were utilized at the generic level. In agreement with previous studies, a rather flattened prothorax where the pronotum is not fused with the prosternum, deflexed pronotal hypomeron, superior marginal line of pronotal hypomeron not distinctly deflected and inferior marginal line not continued as a separate entity beyond anterior pronotal angles, were demonstrated to be plesiomorphic for Staphylinini. The presence of the infraorbital ridge and sexually dimorphic front tarsi have also been shown to be plesiomorphic conditions. Overall, the evolutionary trend in Staphylinini appears to be toward a reduction in the development of the infraorbital ridge coupled with the development of ridges associated with the neck (i.e., dorsal basal ridge, postgenal ridge), a rather convex pronotum that is more integrated with the prosternum, and the reduction of setae on the tarsal segments.

The diversity of Philonthina, the most speciose and derived subtribe of Staphylinini, is here revealed as evolutionary lineages with strong analytical rigour. As suspected, this pattern is only partly congruent with the current generic classification of the subtribe, and in particular it shows that the majority of philonthine diversity was misclassified in large, polyphyletic and poorly diagnosable genera. Based on our total evidence phylogeny, we indicate lineages to which these genera may have to be eventually restricted. Before these taxonomic changes can be made, much taxonomic work in Philonthina is still needed at the species and genus-level. Such taxonomic work may be most efficiently guided by molecular evidence given the high level of morphological homoplasy demonstrated here, and the deeper understanding and modeling of molecular evolution.

Taxonomy

Hyptiomina Casey, 1906

Type genus: *Holisus* Erichson, monotypic.

Diagnosis. *Holisus* can be recognized among all other genera of Staphylinini by the following combination of characters: notably dorso-ventrally flattened body with coarse punctation; last segment of maxillary and labial palps much narrower than penultimate segment; small entire ligula; pronotal hypomera with longitudinal line running between inferior and superior marginal lines (see comments below); anterior tarsi not expanded in both sexes, without adhesive setae ventrally; all tarsi without empodial setae.

Description. Antennae situated at anterior margin of frontoclypeus, i.e., anterior margin of antennal cavity touching anterior margin of frontoclypeus, antennomere 1 as long as or longer than antennomeres 2 and 3 combined, first three antennomeres without tomentose pubescence that starts from antennomere 4. Head with ventral basal ridge along considerable portion of its length confluent with ventral portion of postoccipital suture; postgenal ridge joining ventral basal ridge medially; infraorbital ridges absent; gular sutures joining each other before neck. Ligula small, entire. Apical segments of both maxillary and labial palpi subcylindrical "rod-like", parallel-sided at most of its length, much narrower than penultimate

segment. Mandibles dorso-ventrally flattened, apically sharply pointed, each with one tooth near base. Pronotum with anterior angles not produced beyond anterior margin of prosternum; prosternum with longitudinal ridge; superior marginal line of hypomeron distinctly deflected under anterior angles, inferior marginal line not continued beyond anterior pronotal angles, additional line running on hypomeron between these lines ('c' in fig. 3D in Solodovnikov and Newton, 2005); pronotum and prosternum at least partially fused, pronotosternal suture missing in part of cavity. Elytron without subbasal ridge and evenly punctuate. Mesoscutellum with only anterior scutellar ridge. Mesoventrite with sternopleural (anapleural) suture very slightly oblique, intercoxal process forming obtuse angle. Mesocoxae distinctly recessed compared to metaventrite and intercoxal process, mesocoxae therefore contiguous. Protarsi more or less cylindrical, not transversely widened and not flattened dorso-ventrally, without adhesive setae underneath. Hind wing with veins CuA and MP4 fused in one vein, vein MP3 absent. Male sternum 9 with basal portion either symmetrical or asymmetrical and distal portion acutely emarginate; paramere of aedeagus fused to median lobe only at base but very closely appressed to median lobe along entire length. Female usually with one macroseta at midline of each second gonocoxite.

Comments. The genus *Holisus* is poorly known taxonomically and needs revision. Thirty described species of the genus are confined to the Neotropical region, and only one species, *H. schedli* Scheerpeltz, 1956 (Herman, 2001) was hitherto known from Congo (West Africa). We are aware of two undescribedspecies of *Holisus* in West Africa, also from Congo (Haut Uele and Kalonge respectively), that need further study. One of the morphological characteristics of *Holisus* unique among Staphylinini is the additional longitudinal line (ridge) running on the pronotal hypomeron between the superior and inferior marginal lines. It may well be that it is in fact homologous to the superior marginal line of other Staphylinini, while what appears as a superior line in *Holisus* is in fact a novel structure evolved in connection with strong flattening of the pronotum associated with its subcortical biology. Comparative morphological study of various species of *Holisus* along with a phylogenetic reconstruction of this genus can perhaps shed light on the homology of the pronotal lines in this genus.

Algonina Schillhammer and Brunke, new subtribe

Type genus: *Algon* Sharp

Genera included: *Algon* Sharp and *Barypalpus* Cameron

Diagnosis. Members of Algonina may be recognized among all other subtribes of Staphylinini by the following combination of characters: metacoxae with transverse carinae; all tarsi with empodial setae; and profemora with anterior row of lateroventral spines. The "operculum" situated on the dorsal ostium of the median lobe is a character state unique to Algonina but can only be observed in males.

Description. Antennae with tomentose pubescence starting on antennomere 4 (*Algon*) or 5 (*Barypalpus*), antennomere 3 moderately longer than 2 (a3/a2 ratio 1.2–1.5), antennomere 6 with apical setae (*Algon*) or without (*Barypalpus*). Head with postmandibular ridge separate from mandibular base, with postmandibular sulcus and infraorbital ridge reaching postgenal ridge or slightly extending beyond postgenal ridge, postgenal ridge joining ventral basal ridge medially; ligula small, entire (slightly notched at most); mentum with seta alpha; apical segments of both maxillary and labial palpi fusiform to expanded apically, i.e., narrowed at base but not (or not evenly) converging towards apex; gular sutures not joined before neck, extended slightly separated from each other at base of head capsule; hypostomal cavity distinctly delimited (i.e., cavity surface with microsculpture and/or punctation different from rest of nearby head surface). Disc of neck not distinctly punctate. Prothorax with anterior angles not strongly produced beyond anterior margin of prosternum, disc of pronotum usually impunctate, with long marginal setae not distinct and not regularly distributed, basisternum slightly to moderately longer than furcasternum (bs/fs ratio up to 1.5) with pair of macrosetae situated far from anterior margin of prosternum (i.e., farther than one fourth the distance between the anterior margin and the sternacostal suture along midline); prosternum with microsculpture of oblique and transverse wavelines faint on both basisternum and furcasternum, longitudinal ridge and keel usually absent; superior marginal line of hypomeron not distinctly deflected and large lateral puncture of pronotum situated very close to superior marginal line or at a distance no more than three times its diameter, inferior marginal line not continued as a separate entity beyond anterior pronotal angles. Mesoventrite with sternopleural (anapleural) suture transverse or nearly transverse, more or less straight. Mesocoxae distinctly recessed compared to metaventrite and intercoxal process, mesocoxae therefore contiguous. Profemora with lateroventral apical

spines. Protibiae subconical, moderately broadened apically. Protarsi with tarsomeres 1-4 more or less flattened dorso-ventrally and widened distally with modified (adhesive) pale setae. Mesotarsi with tarsomeres 3-5 glabrous along midline on dorsal surface. Metatibiae spinose. Metatarsi with tarsomere 1 moderately longer than tarsomere 5 (t1/t5 >> 1.0 but < 2.0) and tarsomere 4 with inner marginal spine-like setae. Apical tarsomeres with empodial setae. Hind wing with veins CuA and MP4 completely separate, vein MP3 present, although sometimes faint. Abdomen with prototergal glands as well-developed acetabula; terga 3-5 with pair of accessory ridges on anterior basal transverse carinae only in *Barypalpu*s, sternum 3 with basal transverse carina angulate (*Algon*) or acutely pointed (*Barypalpus*) medially. Apical margin of tergum 8 (bi-) sinuate in *Algon*. Male with patches of setae on disc of sternum 7 only in *Barypalpus*, sternum 9 with basal portion asymmetrical, shorter or as long as distal portion at most (bp/dp 1.0) and distal portion acutely emarginate. Dorsal ostium of median lobe with "operculum" (Schillhammer 2006), conspicuous in both *Algon* (Fig. 7) and *Barypalpus*; paramere of aedeagus fused to median lobe only at base, otherwise paramere distinctly separated from median lobe along entire length, not (or at most slightly) produced over apex of median lobe, paramere narrower than median lobe, with or without sensory peg setae. Female with one macroseta at midline of each second gonocoxite (*Algon*).

Comments. A revision of *Algon* was recently made by Schillhammer (2006, 2008, 2011). We refer the readers to these studies for further details on the genus. The monotypic genus *Barypalpus* Cameron is resurrected from synonymy with *Rientis* Sharp in the present study.

***Barypalpus* Cameron, 1932, stat. resurr.**

Type species: *Barypalpus ruficornis* Cameron, monotypic.

Barypalpus Cameron, 1932: 276 (species included: *ruficornis*); Scheerpeltz, 1933: 1426 (catalog); Blackwelder, 1952: 73 (type species: *ruficornis*); Scheerpeltz, 1962: 265 (characters); Schillhammer, 1999b: 94 (synonym of *Rientis*).

Diagnosis. *Barypalpus* can be recognized -and differs from *Algon*- by the following combination of characters: antennae with antennomere 4 without tomentose pubescence and 6 without apical long setae; abdomen with terga 3-5 with a pair of accessory ridges on each anterior basal transverse carina; male sternum 7 with patches of setae on disc (the latter being the only condition that makes *Barypalpus* different from *Rientis* in this diagnosis, for other characters see diagnosis of Algonina); and posterior margin of tergum 8 evenly rounded, not modified.

Comments. The genus *Barypalpus* was originally described by Cameron (1932) as belonging to "Quediini", then moved to Xanthopygina by Smetana (1977). Schillhammer (1999b) synonymized it with *Rientis* (then also in Xanthopygina) uncritically following a comment in Smetana (1988: 179). Chatzimanolis (2014) removed *Rientis* (including *Barypalpus*) from Xanthopygina and left them as Staphylinini *incertae sedis*. Our study here confirms a sister group relationship of *Barypalpus ruficornis* with *Algon*, which is morphologically supported by three highly homoplastic characters that are not present in *Rientis*: prosternum without keel, mesoventrite with sternopleural (anapleural) suture transverse, or nearly transverse and profemora with lateroventral apical spines (anterior row).

Philonthina Kirby, 1837

Type genus: *Philonthus* Curtis, 1829

Genera included: 73 valid genera (Newton, unpublished database), 57 of them listed in Herman (2001) as valid genera within Philonthina.

Diagnosis. Members of Philonthina can be recognized among other subtribes of Staphylinini by the following combination of characters: apical tarsomere without empodial setae; elytron with subbasal ridge present and sinuate, directed anteriad; mentum with a single seta laterally (setae alpha absent); and dorsal surface of metatarsomeres with only few, marginal setae (except Palaearctic *Jurecekia* Rambousek).

Description. Antennae with tomentose pubescence usually starting on antennomere 4, rarely on antennomere 5. Head with infraorbital ridge variably developed, usually not complete (i.e., reaching

postgenal ridge or extending beyond it); hypostomal cavity absent. Ligula usually small, entire (or at most slightly notched medially). Mentum usually without seta alpha. Neck with transverse carina only within the *Belonuchus* complex (some members), disc of neck impunctate. Prothorax with anterior angles usually not strongly produced beyond anterior margin of prosternum, except some members within the Neotropical lineage; large lateral setiferous puncture either situated very close to superior marginal line of pronotum (or at a distance no more than three times its diameter) or away from it at a distance at least three times as large as its diameter; prosternum with transverse carina on basisternum only within the Neotropical lineage (some members); superior marginal line of hypomeron distinctly deflected under anterior angles (except some myrmecophile genera) and inferior marginal line not continued as a separate entity beyond anterior pronotal angles. Mesoventrite with sternopleural (anapleural) suture transverse, or nearly transverse (very slightly oblique) or distinctly oblique (medial end of suture anterior to its lateral end), only confluent at anterior margin of mesoventrite within the *Belonuchus* complex (some members); posterior half of prepectus usually with a ridge connecting coxal cavities, except *Eccoptolonthus* and one species in the *Belonuchus rufipennis* group. Profemora spinose or not. Protibiae variably shaped, mostly cylindrical or subconical, distinctly broadened and flattened laterally in *Thinocafius*, with apical excavation only within the *Belonuchus* complex (some members). Protarsi sexually dimorphic or not. Metatarsi with tarsomeres 3-5 glabrous along midline on dorsal surface, except *Jurecekia*. Metacaoxae usually with ventral spines. Metatibiae spinose or not. Apical tarsomeres without empodial setae, with empodial spine in myrmecophile genera. Hind wing with veins CuA and MP4 fused into one vein (although often its origin from two veins still very obvious), usually with vein MP3, although sometimes faint. Abdomen with prototergal glands developed as more or less invaginated capsules with smaller openings, except *Philonthus caeruleipennis*; abdominal tergites often with posterior transverse basal line; sternum 3 with basal transverse carina variably shaped in medial area, mostly straight to arcuate. Male sternum 9 with basal portion either more or less symmetrical (i.e., both lateral ends similarly produced, not extending far from each other) or asymmetrical (i.e., one lateral end distinctly produced, extending far from the other). Paramere of aedeagus fused to median lobe only at base, not (or at most slightly) produced over apex of median lobe or distinctly small (short and/or thin), with or without sensory peg setae.

Note. *Endeius ovaliceps* Coiffait, a species from San Cristobal (Galapagos Islands) considered exceptional among Philonthina in having empodial setae, and transferred to the genus *Philonthus* in Chani-Posse (2013), in fact belongs to the subtribe Amblyopinina. Generic assignment of that species within Amblyopinina is problematic and will be dealt in a separate paper soon.

***Belonuchus* Nordmann**

Type species: *Staphylinus haemorrhoidalis* Fabricius

Species included: the nine species listed by Smetana (1995) plus *B. haemorrhoidalis* (Fabricius) and *B. pollens* Sharp (from our study). There are additional species currently placed in *Belonuchus* that, according to this study, do not belong to the genus but are not yet placed elsewhere.

Diagnosis. Species of this group can be recognized among other genera of Philonthina by the following characters: head without postmandibular ridge; with infraorbital ridge reaching postgenal ridge or slightly extending beyond postgenal ridge; gular sutures joined anteriorly before neck; mesothorax with sternopleural (anapleural) suture transverse, or nearly transverse (very slightly oblique); profemora with two rows of lateroventral spines; protarsi not sexually dimorphic, tarsomeres 1-4 more or less cylindrical, not transversely widened and not flattened dorso-ventrally, without modified (pale) adhesive setae; and abdominal terga 3-5 with posterior basal transverse carina.

Description. Antennae situated closer to frontoclypeus than to eyes, with tomentose pubescence starting on antennomere 4. Head without postmandibular ridge, with infraorbital ridge reaching postgenal ridge or slightly extending beyond postgenal ridge; gular sutures joined anteriorly before neck. Labial palpi with apical segment fusiform, distinctly longer than preceding segment. Maxillary palpi with apical segment either fusiform or subcylindrical. Neck without transverse carina. Prothorax with anterior angles not strongly produced beyond anterior margin of prosternum; large lateral setiferous puncture usually situated away from it at a distance at least three times as large as its diameter; prosternum with transverse carina on basisternum, usually rudimentary to uncomplete; basisternum with pair of macrosetae situated close to anterior margin of prosternum (i.e., not farther than one fourth the distance between amp and the ss along midline). Mesoventrite with sternopleural (anapleural) suture transverse, or nearly transverse (very slightly

oblique); posterior half of prepectus usually with a ridge connecting coxal cavities; intercoxal process usually rounded or broadly pointed, forming obtuse angle, rarely metaventrite fused with mesoventrite, so not distinct. Profemora with apical (anterior row) and medial (posterior row) lateroventral spines. Protibiae cylindrical to subconical, without apical excavation. Protarsi not sexually dimorphic, tarsomeres 1-4 more or less cylindrical, not transversely widened and not flattened dorso-ventrally, without modified (pale) adhesive setae. Metacoxae with ventral spines. Metafemora sexually dimorphic or not, if so, spinose on males. Metatibiae spinose. Abdomen with terga 4 and 5 with posterior basal transverse carina; sternum 3 with basal transverse carina straight to arcuate medially. Male sternum 9 with basal portion slightly to moderately asymmetrical (i.e., one lateral end distinctly produced, extending far from the other). Paramere of aedeagus fused to median lobe only at base, distinctly small (short and/or thin), without sensory peg setae.

Comments. The concept of *Belonuchus* defined herein is in agreement with that of Smetana (1995) and Chani-Posse (2014a). However, the majority of species currently described in *Belonuchus* do not fit this concept and need to be placed elsewhere.

Trapeziderus Motschulsky, 1860, stat. resurr.

Type species: *Trapeziderus bicolor* Motschulsky, fixed by monotypy.

Trapeziderus Motschulsky, 1860a: 77 (species included: *bicolor*); Gemminger and Harold, 1868: 599 (catalog); Fauvel, 1895: 266 (synonym of *Belonuchus*); Bernhauer and Schubert, 1914: 369 (synonym of *Belonuchus*); Cameron, 1932: 170 (synonym of *Belonuchus*); Blackwelder, 1943: 420 (synonym of *Belonuchus*; type species: *bicolor*); Blackwelder, 1952: 392 (synonym of *Belonuchus*; type species: *bicolor*); Smetana, 1995: 722 (synonym of *Belonuchus*).

Trapezinotus Motschulsky, 1870: 49 (species included: *bicolor*; cited with *Trapeziderus* as junior synonym. According to Herman (2001), this name was cited as the senior synonym of *Trapeziderus*, though this action was not justified.

Species included: Fifty-five species are included herein, after being transferred to *Trapeziderus* from *Belonuchus* (38 spp.), *Hesperus* (16 spp.) and *Philonthus* (1 sp.). The following species are transferred from *Belonuchus* to *Trapeziderus* and are **new combinations**: *T. abdominalis* (Cameron), *T. anthracinus* (Schubert), *T. assamensis* (Cameron), *T. associatus* (Cameron), *T. bafutensis* (Levasseur), *T. bakeri* (Bernhauer), *T. bicoloratus* (Schubert), *T. bicoloripennis* (Bernhauer), *T. birmanus* (Cameron), *T. borneensis* (Cameron), *T. brevicollis* (Fauvel), *T. ceylonicus* (Cameron), *T. coomani* (Li & Zhou), *T. diversus* (Bernhauer), *T. ferrugatus* (Erichson), *T. fuscipes* (Fauvel), *T. grandiceps* (Kraatz), *T. grandis* (Bernhauer), *T. imitator* (Cameron), *T. imperialis* (Cameron), *T. javanus* (Cameron), *T. kedirianus* (Cameron), *T. lividipes* (Fauvel), *T. mutator* (Fauvel), *T. nigrorufus* (Fauvel), *T. nilgiriensis* (Cameron), *T. obscuricornis* (Bernhauer), *T. obvelatus* (Li & Zhou), *T. parcus* (Bernhauer), *T. picticollis* (Cameron), *T. punctus* (Schubert), *T. quadratus* (Kraatz), *T. quadriceps* (Fauvel), *T. ruficeps* (Cameron), *T. rufoniger* (Fauvel), *T. semitestaceus* (Schubert), *T. subdentatus* (Eppelsheim) and *T. taprobanus* (Cameron). The following species are transferred from *Hesperus* to *Trapeziderus* and are **new combinations**: *T. addisadebaensis* (Scheerpeltz), *T. africanus* (Bernhauer), *T. anas* (Hromádka), *T. belonuchiformis* (Bernhauer), *T. burgeoni* (Bernhauer), *T. cafioides* (Fauvel), *T. depressus* (Bernhauer), *T. fraternus* (Bernhauer), *T. gridellianus* (Bernhauer), *T. kraatzi* (Eppelsheim), *T. mirus* (Bernhauer), *T. nobilis* (Bernhauer), *T. oriolus* (Hromádka), *T. sericeicoicollis* (Cameron), *T. sparsior* (Bernhauer) and *T. spectabilis* (Bernhauer). One species is transferred from *Philonthus* to *Trapeziderus* with the following **new combination**: *T. macrocephalus* (Sharp).

Diagnosis. *Trapeziderus* can be recognized by the following combination of characters: head without infraorbital ridge; gular sutures joined anteriorly (i.e., not farther than one half the distance between the anterior margin of mentum and the base of head along midline); usually with crescent-shaped temporal carina; prosternum with pair of macrosetae of basisternum situated close to anterior margin of prosternum; protarsi with tarsomeres 1-4 more or less flattened dorso-ventrally and widened distally with modified (adhesive) pale setae; mesotobia with very long and thin seta mesolaterally; abdominal sternum 3 with basal transverse carina straight to arcuate on medial area.

Comments. The genus *Trapeziderus* was originally described by Motschulsky (1860) and was later (1870) treated as a junior synonym of *Trapezinotus* Motschulsky, 1870 by the same author, for unclear reasons (Herman 2001). However, this unjustified action was not followed by later authors such as Fauvel (1895) who synonymized *Trapeziderus* with *Belonuchus* (senior synonym), an arrangement which has persisted until this study. Although *Trapeziderus* and *Belonuchus* share many characters given in the current diagnosis, they can be easily differentiated by the configuration of the protarsi and the well developed paramere of the aedeagus, which usually bears peg setae on its underside. In *Belonuchus* the paramere is distinctly small (short and/or thin) and without sensory peg setae. These differences were recognized earlier by Li and Zhou (2010, 2011).

Other taxonomic changes affecting Philonthina

We refer the readers to Herman (2001) for further references on the following names.

Eccoptolonthus laevigatus (Fauvel), **comb. nov.**
Eccoptolonthus roepkei (Bernhauer), **comb. nov.**

Comments. Our decision to transfer these two species from *Hesperus* to *Eccoptolonthus* is supported by both molecular and morphological data. Both species and *Eccoptolonthus* have protarsomeres 1-4 that are more or less cylindrical, not transversely widened, not flattened dorso-ventrally, and lack modified (pale) adhesive setae, while true species of *Hesperus* have protarsomeres 1-4 that are more or less flattened dorso-ventrally and widened distally with modified (adhesive) pale setae. Additionally, a mesoventral anterior carina of prepectus has been shown to be unique to *Eccoptolonthus* in the present study.

Paederomimus mimeticus (Sharp), **comb. nov.**

Comments. Although the monophyly of *Paederomimus* was not confirmed in the present study, *Belonuchus mimeticus* Sharp does not fit into the definition of *Belonuchus* (see above) and it appears nested within the major *Paederomimus* subclade, which includes all but one of the *Paederomimus* representatives considered herein. Furthermore, it fits the morphological diagnosis of *Paederomimus* given by Chani-Posse (2014a).

Pridonius Blackwelder, **stat. nov.**
Type species: *Pridonius iheringi* (Bernhauer) designated by Blackwelder (1952), **comb. nov.**

Species included: *Pridonius iheringi* (Bernhauer) and *P. sparsiventris* (Bernhauer), both **comb. nov.**

Comments. *Pridonius iheringi* is moved from Quediina to Philonthina based on our current results, which show that this species is closely related to other myrmecophile genera within the Neotropical lineage of Philonthina. Our results corroborate those of Brunke and Solodovnikov (2013), where any similarity of *Pridonius* to *Quedius* was shown to be related mostly to its broad and flattened habitus.

Philothalpina Chatzimanolis and Brunke, new subtribe

Type genus: *Philothalpus* Kraatz, monotypic

Diagnosis. Philothalpina can be recognized among other subtribes of Staphylinini by the following combination of characters: metacoxae with transverse ridge; apical tarsomere with empodial setae; ridge on posterior half of mesoventrite present with distinct lateral arms extending to mid-width of mesocoxal cavities (Fig. 8A); sternopleural (anapleural) suture of mesoventrite distinctly sinuate (Fig. 8A). Philothalpina are most likely to be confused with Xanthopygina but can easily be distinguished by the pair accessory ridges on the anterior basal transverse carina (Fig. 8B) or the extremely wide lateral arms of the basisternum, which are distinctly more than 1.5 times the width of the furcasternum (Fig. 8A).

Description. Antennae with tomentose pubescence starting on antennomere 4. Head with postmandibular ridge separated from mandibular base; with postmandibular sulcus and infraorbital ridge reaching postgenal ridge or slightly extending beyond postgenal ridge; hypostomal cavity slightly delimited (cavity distinct only laterally, its surface with same microsculpture or punctation as rest of nearby head surface); gular sutures not joined before neck and slightly separated from each other. Ligula small, entire (slightly notched at most). Mentum with seta alpha. Disc of neck impunctate. Prothorax with anterior angles not produced beyond anterior margin of prosternum; prosternum with lateral areas of basisternum distinctly longer than those of furcasternum (Fig. 8A); postcoxal process absent; superior marginal line of hypomeron not deflected under anterior angles and inferior marginal line not curving around anterior angles as a separate entity as in Xanthopygina. Mesoventrite with sternopleural (anapleural) suture sinuate; mesocoxae distinctly recessed compared to metaventrite but on approximately same plane as intercoxal process, mesocoxae therefore moderately separated; intercoxal process narrowly pointed forming sharp (acute) angle. Profemora not spinose. Protibiae subconical. Protarsi sexually dimorphic, tarsomeres 1-4 more or less flattened dorso-ventrally and widened distally, with modified (pale) adhesive setae. Metatarsomeres 3-5 dorsally setose (except *P.fervidus* and *P. rugosus*, which bear only a few scattered setae on each disc). Metacoxae with transverse carina and ventral spines. Metatibiae spinose or not. Apical tarsomeres with empodial setae. Hind wing with veins CuA and MP4 fused in one vein (although often its origin from two veins still very obvious), with vein MP3, although sometimes faint. Abdomen with prototergal glands as well developed acetabula. Abdominal terga 3-5 without posterior basal transverse carina, terga 3 and 4 each with a pair of accessory ridges on the anterior basal transverse carina (Fig. 8B); sternum 3 with basal transverse carina acutely pointed medially. Male sternum 7 with patch of setae on disc. Male sternum 9 with basal portion asymmetrical and distal portion distinctly emarginate. Paramere of aedeagus fused to median lobe only at base, not (or at most slightly) produced over apex of median lobe, with sensory peg setae.

Comments. A revision and phylogeny of *Philothalpus* was produced by Chatzimanolis and Ashe (2005). The concept of *Philothalpus* defined herein is in agreement with that of these authors and we refer the readers to this study for further details on the genus.

Staphylinina Latreille, 1802
Eucibdelina Sharp, 1889, **syn. nov.**

Type genus: *Staphylinus* Linnaeus

Genera included: 48 genera listed in Staphylinina (plus Eucibdelina) (Newton, unpublished database).

Diagnosis. Members of Staphylinina can be recognized among other subtribes of Staphylinini by the following combination of characters: head with ligula more or less bilobed; superior marginal line of hypomeron deflected under anterior angles and inferior marginal line usually not continued as a separate entity beyond anterior pronotal angles, otherwise (rarely) continued as a separate entity beyond anterior pronotal angles and continuous with them (*Creophilus* complex); protarsomeres 1-4 more or less flattened dorso-ventrally and widened distally, with modified (pale) adhesive setae; mesotarsomeres dorsally setose (setae not restricted to marginal series); abdomen with prototergal glands developed as shallow impressions and terga 3-5 without posterior basal transverse carina.

Description. Antennae with tomentose pubescence starting on antennomere 4 or 5. Head with postmandibular ridge absent or present, if so, usually separated from mandibular base or bordering it only laterally (*Rhyncocheilus*); usually with postmandibular sulcus (absent in *Rhyncocheilus*) and infraorbital ridge usually reaching postgenal ridge or slightly extending beyond postgenal ridge (absent in *Rhyncocheilus*); hypostomal cavity distinctly delimited (i.e., cavity surface with microsculpture and/or punctation different from rest of nearby head surface); gular sutures not joined before neck and slightly separated from each other. Ligula bilobed. Mentum with seta alpha. Disc of neck either punctate or impunctate. Prothorax with anterior angles not produced beyond anterior margin of prosternum; postcoxal process present or absent; superior marginal line of hypomeron deflected under anterior angles and inferior marginal line usually not continued as a separate entity beyond anterior pronotal angles, rarely continued as a separate entity beyond anterior pronotal angles and continuous with them. Mesoventrite with sternopleural (anapleural) suture transverse or distinctly oblique; mesocoxae either distinctly recessed compared to metaventrite but on approximately same plane as intercoxal process, mesocoxae therefore moderately separated or not and on approximately same plane as intercoxal process and

metaventrite, mesocoxae therefore at least narrowly separated; intercoxal process narrowly pointed forming sharp (acute) angle or rounded to broadly pointed, forming obtuse angle. Profemora not spinose. Protibiae usually subconical, or extremely dilated (some members of the Eucibdelus lineage). Protarsi sexually dimorphic, tarsomeres 1-4 more or less flattened dorso-ventrally and widened distally, with modified (adhesive) pale setae. Metatarsomeres 3-5 dorsally setose (setae not restricted to marginal series). Metacoxae usually with transverse carina and ventral spines. Metatibiae usually spinose, rarely with one or two spines at most (*Rhyncocheilus*). Apical tarsomeres with empodial setae. Hind wing with veins CuA and MP4 separate, usually with vein MP3, although sometimes faint. Abdomen with prototergal glands developed as shallow impressions. Abdominal terga 3-5 without posterior basal transverse carina; sternum 3 with basal transverse carina variably shaped. Male sternum 9 with basal portion asymmetrical (i.e., one lateral end distinctly produced, extending far from the other) and distal portion distinctly emarginate. Paramere of aedeagus fused to median lobe only at base, not (or at most slightly) produced over apex of median lobe, with or without sensory peg setae.

Comments. The subtribe Eucibdelina Sharp is synonymized with the subtribe Staphylinina Latreille in the present study. Herman (2001) as well as Newton and Thayer (2005) already considered genera of Eucibdelina as part of Staphylinina, while Bouchard *et al.* (2011) recognized Eucibdelina as valid subtribe within Staphylinini.

Xanthopygina Sharp, 1884

Type genus: *Xanthopygus* Kraatz

Genera included: 29 genera: *Darwinilus* Chatzimanolis, *Dysanellus* Bernhauer, *Elecatopselaphus* Scheerpeltz, *Elmas* Blackwelder, *Gastrisus* Sharp, *Glenus* Kraatz, *Haematodes* Laporte, *Isanopus* Sharp, *Nausicotus* Sharp, *Nordus* Blackwelder, *Ocyolinus* Sharp, *Oligotergus* Bierig, *Paraxenopygus* Bernhauer, *Phanolinopsis* Scheerpeltz, *Phanolinus* Sharp, *Plociopterus* Kraatz, *Scaponopselaphus* Sharp, *Scariphaeus* Erichson, *Smilax* Laporte, *Styngetus* Sharp, *Terataki* Chatzimanolis, *Torobus* Herman, *Triacrus* Nordmann, *Tricholinus* Bernhauer, *Trigonopselaphus* Gemminger and Harold, *Xanthopygus* Kraatz, *Xenopygus* Bernhauer, *Weiserianum* Bernhauer, *Zackfalinus* Chatzimanolis.

Diagnosis. Members of Xanthopygina can be recognized among other subtribes of Staphylinini by the following combination of characters: head with dorsal basal ridge; apical tarsomeres with empodial setae; metatarsomeres 3-5 glabrous along midline on dorsal surface; nearly all genera with inferior marginal line continued beyond anterior angles as a separate entity and curving around them; abdominal tergites never with accessory lines on anterior transverse basal line but often with separate curved lines posteriad of the latter structure.
The larvae of Xanthopygina possess distinctive, long urogomphi.

Description. Antennae with tomentose pubescence starting on antennomere 4 or 5. Head with postmandibular ridge separated from mandibular base; with or without postmandibular sulcus and infraorbital ridge usually reaching postgenal ridge or slightly extending beyond postgenal ridge, rarely extending far beyond postgenal ridge (e.g., *Glenus*); gular sutures not joined before neck and slightly separated from each other. Ligula small, entire (slightly notched at most), rarely bilobed (*Xanthopygus*). Mentum with seta alpha. Disc of neck usually impunctate. Prothorax with postcoxal process present or absent; superior marginal line of hypomeron not deflected under anterior angles and inferior marginal line usually continued as a separate entity beyond anterior pronotal angles and curving around them. Mesothorax with sternopleural (anapleural) suture transverse or distinctly oblique; mesocoxae distinctly recessed compared to metaventrite but on approximately same plane as intercoxal process, mesocoxae therefore moderately separated; mesothorax with intercoxal process narrowly pointed forming sharp (acute) angle or rounded to broadly pointed, forming obtuse angle. Profemora not spinose. Protibiae usually subconical, except in myrmecophilous taxa. Protarsi usually sexually dimorphic, tarsomeres 1-4 more or less flattened dorso-ventrally and widened distally, with modified (adhesive) pale setae. Metatarsomeres 3-5 glabrous along midline on dorsal surface. Metacaoxae with transverse carina and ventral spines. Apical tarsomeres with empodial setae. Hind wing with veins CuA and MP4 fused in one vein (although often its origin from two veins still very obvious), with vein MP3, although sometimes faint. Abdomen with prototergal glands as well developed acetabula. Abdominal terga 3-5 without posterior basal transverse carina; sternum 3 with basal transverse carina angulate or acutely pointed medially. Sternites 7 and 8 typically sexually dimorphic; male sternite 7 sometimes with porose structure

(=patch of setae on disc) or modified posterior margin (projection or emargination); male sternite 8 usually with modified posterior margin (projection or emargination); male sternite 9 with basal portion more or less symmetrical and distal portion distinctly emarginate. Paramere of aedeagus with or without sensory peg setae.

Acknowledgments

We thank Al Newton, Margaret Thayer, Steve Marshall and Steve Paiero for providing DNA-grade specimens for study. These and many more colleagues listed in the Methods section are thanked for providing specimens that were used for our ongoing morphological research. The first author (MRCP) is especially indebted to the Biosystematics Department and the molecular laboratory at the Natural History of Denmark (ZMUC) where most of the data for this paper have been generated during her one year stay at this institution. In particular, Andrea Schomann, then graduate student at ZMUC, is sincerely acknowledged for providing training on molecular techniques. MRCP is also thankful to Federico Agrain and Germán San Blas for our constructive talks concerning cladistic analyses. Funding for this project was provided by CONICET, Argentina (Becas externas para jóvenes investigadores) (to MRCP), by the University of Copenhagen, and by the Carlsberg Foundation (funds for molecular work and collecting expeditions granted to AS). This research also received support from Ernst Mayr Travel Grant (MCZ, Harvard University) to MRCP. AJB received support from a fellowship (with N. Akkari, Natural History Museum of Vienna) from the European Union's Horizon 2020 research and innovation programme under the Marie Sklodowska-Curie grant agreement No 642241 (BIG4). SC was partially funded by NSF DEB 0741475 (to S. Chatzimanolis and M. S. Engel) and by a Research and Creative Activity Award from the College of Arts and Sciences at the University of Tennessee at Chattanooga. We thank the Willi Hennig Society (cladistics.org) for making TNT freely available and the CIPRES Scientific Gateway for access to computational resources. Thanks to Adam Bazinet and Derrick Zwickl for their assistance with GARLI, also to M.E. Smirnov (St. Petersburg, Russia) and K.V. Makarov (Moscow, Russia) for the use of their habitus photographs available from www.zin.ru/animalia/coleoptera. The authors declare that there are no conflicts of interest.

References

Asenjo, A., Ribeiro-Costa, C. S. 2009. Two new species of the Neotropical genus *Philothalpus* Kraatz from Peru (Coleoptera, Staphylinidae, Xanthopygina). Zootaxa 2286, 49–57.

Assing, V. 2015. A new species of *Algon* from Vietnam. Linzer Biol. Beitr. 47(2), 1251–1256.

Assis, L. C. S. 2015. Homology assessment in parsimony and model-based analyses: two sides of the same coin. Cladistics 31, 315–320. doi: 10.1111/cla.12085

Bazinet, A., Zwickl, D., Cummings, M. 2014. A Gateway for Phylogenetic Analysis Powered by Grid Computing Featuring GARLI 2.0. Syst. Biol. 63, 812–818.

Bergsten, J. 2005. A review of long-branch attraction. Cladistics 21, 163–193.

Bernhauer, M., Schubert, K. 1914. Staphylinidae IV. In: Schenkling, S. (Ed.), Coleopterorum Catalogus. Pars 57. W. Junk, Berlin, pp. 289–408.

Blackwelder, R. E. 1936. Morphology of the coleopterous family Staphylinidae. Smith. Misc. Coll. 94(13), 1–102.

Blackwelder, R. E. 1943. Monograph of the West Indian beetles of the family Staphylinidae. U. S. Natl. Mus. Bulletin 182 (i–viii), 1–658.

Blackwelder, R. E. 1952. The generic names of the beetle family Staphylinidae, with an essay on genotypy. U. S. Natl. Mus. Bulletin 200(i–iv), 1–483.

Bouchard, P., Bousquet, Y., Davies, A. E., Alonso-Zarazaga, M. A., Lawrence, J. F., Lyal, C. H. C.,

Newton, A. F., Reid, C. A. M., Schmitt, M., Ślipiński, A. and Smith, A. B. T. 2011. Family-group names in Coleoptera (Insecta). ZooKeys 88, 1–972.

Brunke, A., Solodovnikov, A. 2013. *Alesiella* gen.n. and a newly discovered relict lineage of Staphylinini (Coleoptera: Staphylinidae). Syst. Entomol. 38, 689–707.

Brunke, A., Solodovnikov, A. 2014. A revision of the Neotropical species of *Bolitogyrus* Chevrolat, a geographically disjunct lineage of Staphylinini (Coleoptera, Staphylinidae). ZooKeys 423, 1–113.

Brunke, A. J., Chatzimanolis, S., Schillhammer, H., Solodovnikov, A. 2016. Early evolution of the hyperdiverse rove beetle tribe Staphylinini (Coleoptera: Staphylinidae: Staphylininae) and a revision of its higher classification. Cladistics 32, 427–451. doi: 10.1111/cla.12139

Bukontaite, R., Miller, K., Bergsten, J. 2014. The utility of CAD in recovering Gondwanan vicariance events and the evolutionary history of Aciliini (Coleoptera: Dytiscidae). BMC Evol. Biol. 14, 1–18.

Cai, C. Y., Newton, A. F., Huang, D. Y., Tang, L. 2014. A new species of *Platydracus* Thomson, 1858 (Coleoptera, Staphylinidae, Staphylininae) from the upper Eocene Florissant beds, Colorado, USA. Palaeoworld 23, 321–326.

Cameron, M. 1932. Coleoptera, Staphylinidae. Vol. III. In: Stephenson, J. (Ed.), Fauna of British India, including Ceylon and Burma. Taylor & Francis, London. xiii + 443 pp., pls. 1-2.

Cecca, F., Azema, J., Fourcade, E., Baudin, F., Guiraud, R., De Wever, P. 1993. Early Kimmeridgian palaeoenvironments (146–144 Ma). In: Dercourt, J., Ricou, L. E., Vrielynck, B. (Eds.), Atlas Tethys Palaeoenvironmental Maps. Gauthier-Villars, Paris, France, pp. 307.

Chani-Posse, M. 2010. Revision of the southern South American species of *Philonthus* Stephens (Coleoptera: Staphylinidae). Zootaxa 2595, 1–70.

Chani-Posse, M. 2013. Towards a natural classification of the subtribe Philonthina (Coleoptera: Staphylinidae: Staphylinini): a phylogenetic analysis of the Neotropical genera. Syst. Entomol. 38, 390–406.

Chani-Posse, M. 2014a. An illustrated key to the New World genera of Philonthina Kirby (Coleoptera: Staphylinidae), with morphological, taxonomical and distributional notes. Zootaxa 3755(1), 62–86.

Chani-Posse, M. 2014b. Systematics and phylogeny of the Neotropical genera *Pescolinus* Sharp and *Neopescolinus* gen.n. (Coleoptera: Staphylinidae). Arthropod Syst. Phylo. 72(3), 237–255.

Chani-Posse, M., Asenjo, A. 2013. Systematics and phylogeny of the Andean genera *Leptopeltus* Bernhauer and *Leptopeltoides* gen. nov. (Coleoptera: Staphylinidae), with biogeographical notes. Zool. Anz. 252 (4), 440–456.

Chani Posse, M., Couturier, G. 2012. *Delgadobius amazonensis*—a new genus and species of the subtribe Philonthina from Amazonia (Coleoptera: Staphylinidae: Staphylininae). Zootaxa 3568, 81–88.

Chani-Posse, M., Newton, A. F. 2015. *Flohria* Sharp - a Relictual Genus of the Subtribe Philonthina From the Americas (Coleoptera: Staphylinidae: Staphylininae). Ann. Entomol. Soc. America 108 (3), 372–382.

Chatzimanolis, S. 2014. Phylogeny of xanthopygine rove beetles (Coleoptera) based on six molecular loci. Syst. Entomol. 39, 141–149.

Chatzimanolis, S., Ashe, J. S. 2005. Revision and phylogeny of the Neotropical genus *Philothalpus* (=*Eugastus* Sharp and *Allostenopsis* Bernhauer) (Coleoptera: Staphylinidae: Xanthopygina). Insect Syst. Evol. 36, 63–119.

Chatzimanolis, S., Chani-Posse, M. 2016. On the myrmecophilous species of Plociopterus Kraatz described by Wasmann (Coleoptera: Staphylinidae: Staphylinini). Coleopt. Bull., 70(2), 214–216.

Chatzimanolis, S., Cohen, I. M., Schomann, A. S., Solodovnikov, A. 2010. Molecular phylogeny of the mega-diverse rove beetle tribe Staphylinini (Insecta, Coleoptera, Staphylinidae). Zool. Scr. 39, 436–449.

Clarke, D. J. 2011. Testing the phylogenetic utility of morphological character systems, with a revision of *Creophilus* Leach (Coleoptera: Staphylinidae). Zool. J. Linn. Soc. 163(3), 23–812.

Erixon, P., Svennblad, B., Britton, T., Oxelman, B. 2003. Reliability of Bayesian Posterior Probabilities and Bootstrap Frequencies in Phylogenetics. Syst. Biol. 52, 665–673.

Fauvel, A. 1895. Staphylinides nouveaux de l' Inde et de la Malaisie. Revue d' Entomologie 14, 180–286.

Frank, J. H., Barrera, R. 2010. Natural history of *Belonuchus* Nordmann spp. and allies (Coleoptera: Staphylinidae) in *Heliconia* L. (Zingiberales: Heliconiaceae) flower bracts. Insecta Mundi 110, 1–12.

Friis, E. M., Crane, P. R., Raunsgaard Pedersen, K. 2011. Early Flowers and Angiosperm Evolution. 1st ed. Cambridge: Cambridge University Press Cambridge Books Online. http://dx.doi.org/10.1017/CBO9780511980206

Gemminger, M., von Harold, E. 1868. Catalogus Coleopterorum hucusque descriptorum synonymicus et systematicus. Vol. 2. Dytiscidae, Gyrinidae, Hydrophilidae, Staphylinidae, Pselaphidae, Gnostidae, Paussidae, Scydmaenidae, Silphidae, Trichopterygidae, Scaphidiidae. E. H. Gummi, Monachii [Munich]. pp. 425–752 + 6 unnumbered [Index].

Goloboff, P. A., Farris, J. S., Källersjö, M., Oxelman, B., Ramírez, M. J., Szumik, C. A. 2003. Improvements to resampling measures of group support. Cladistics 19, 324–332.

Goloboff, P., Carpenter, J., Arias, S., Miranda, D., 2008a. Weighting against homoplasy improves phylogenetic analysis of morphological data sets. Cladistics 24, 758–773.

Goloboff, P. A., Farris, J. S., Nixon, K. C. 2008b. TNT, a free program for phylogenetic analysis. Cladistics 24, 774–786.

Hayashi, Y. 1993. Studies on the Asian Staphylinidae, I (Coleoptera, Staphylinidae). Elytra 21, 281–301.

Hayashi, Y. 2005. Studies on the Asian Staphylinidae, VI (Coleoptera, Staphylinidae). Elytra 33, 547–560.

Hayashi, Y. 2011. A new species of *Algon* (Coleoptera, Staphylinidae) from China, with some notes on the generic characteristics. Elytra, Tokyo, New Series 1 (1), 67–72.

Herman, L. 2001. Catalog of the Staphylinidae (Insecta, Coleoptera): 1758 to the end of the second millennium. Bull. Am. Mus. Nat. Hist. 265, 4218 p.

Hillis, D. M., Wiens, J. J. 2000. Molecular versus morphological systematics: Conflicts, artifacts, and misconceptions. Pages 1–19 in Phylogenetic analysis of morphological data (J. J. Wiens, ed.). Smithsonian Institution Press, Washington, D.C.

Hromádka, L. 2008a. Revision of Afrotropical species of the *Philonthus abyssinus* species group (Coleoptera: Staphylinidae: Philonthina). Acta Entomol. Mus. Natl. Pragae 48, 37–50.

Hromádka, L. 2008b. Revision of Afrotropical species of the *Philonthus peripateticus* species group (Coleoptera: Staphylinidae: Philonthina). Acta Entomol. Mus. Natl. Pragae 48 51–65.

Hromádka, L. 2009. Revision of the Afrotropical species of the *Philonthus caffer* species group (Coleoptera: Staphylinidae: Philonthina). Acta Entomol. Mus. Natl. Pragae 49, 161–190.

Hromádka, L. 2010a. A revision of the Afrotropical species of the *Philonthus arrowianus* species group (Coleoptera: Staphylinidae: Philonthina). Acta Entomol. Mus. Natl. Pragae 50, 131–144.

Hromádka, L. 2010b. Revision of Afrotropical species of the *Philonthus aemulus* species group (Coleoptera: Staphylinidae: Philonthina). Acta Soc. Zool. Bohem. 73(1–2), 27–51.

Hromádka, L. 2010c. Revision of the Afrotropical species of the *Philonthus marginipennis* species group (Coleoptera: Staphylinidae: Philonthina). Acta Soc. Zool. Bohem. 73(1–2), 53–64.

Jeon, M.-J., Song, J.-H., Ahn, K.-J. 2012. Molecular phylogeny of the marine littoral genus *Cafius* (Coleoptera: Staphylinidae: Staphylininae) and implications for classification. Zool. Scr. 41, 150–159.

Katoh, K., Misawa, K., Kuma, K., Miyata, T. 2002. MAFFT: a novel method for rapid multiple sequence alignment based on fast Fourier transform. Nucleic Acids Research 30, 3059–3066.

Lanfear, R., Calcott, B., Ho, S., Guindon, S. 2012. PartitionFinder: combined selection of partitioning schemes and substitution models for phylogenetic analyses. Mol. Biol. Evol. 29, 1695–1701.

Lewis, P. O. 2001. A likelihood approach to estimating phylogeny from discrete morphological character data. Syst. Biol. 50(6), 913–925.

Lopardo, L., Giribet, G., Hormiga, G. 2011. Morphology to the rescue: molecular data and the signal of morphological characters in combined phylogenetic analyses—a case study from mysmenid spiders (Araneae, Mysmenidae), with comments on the evolution of web architecture. Cladistics 27, 278–330.

Li, L., Zhou, H.-Z. 2010. Revision of the Chinese species of the genus *Belonuchus* Nordmann (Coleoptera: Staphylinidae: Philonthina). J. Nat. Hist. 44, 2149–2177.

Li, L., Zhou, H.-Z. 2011. Revision and phylogenetic assessment of the rove beetle genus *Eccoptolonthus* Hayashi, with broad reference to the subtribe Philonthina (Coleoptera: Staphylinidae: Staphylinini). Zool. J. Linn. Soc. 163, 679–722.

Maddison, D. R. 2012. Phylogeny of *Bembidion* and related ground beetles (Coleoptera: Carabidae: Trechinae: Bembidiini: Bembidiina). Mol. Phylogenet. Evol. 63, 533–576.

Maddison, W., Maddison, D. R. 2015. Mesquite: A modular system for evolutionary analyses. Version 3.01. Published by the authors. <http://mesquiteproject.org/mesquite/mesquite.html>.

Motschulsky, V. 1860. Entomologie spéciale. Insectes des Indes orientales, et de contrées analogues. Etud. Entomol. 8, 25–118.

Motschulsky, V. 1870. Genres et espèces d'insectes, publiés dans différents ouvrages par Victor Motschoulsky. Hor. Soc. Ent. Ross. 6 (supplément), 47–118.

Naomi, S. I. 1987a. Comparative Morphology of the Staphylinidae and the Allied Groups (Coleoptera, Staphylinoidea) I. Introduction, Head Sutures, Eyes and Ocelli. Kontyû 55(3), 450–458.

Naomi, S. I. 1987b. Comparative Morphology of the Staphylinidae and the Allied Groups (Coleoptera, Staphylinoidea) II. Cranial Structure and Tentorium. Kontyû 55(4), 666–675.

Newton, A. F. 1988. Fooled by flatness: subfamily shifts in subcortical Staphylinidae (Coleoptera). Coleopt. Bull. 42(3), 255–262.

Newton, A. F., Jr., Thayer, M. K. 1992. Current classification and family-group names in Staphyliniformia (Coleoptera). Fieldiana: Zoology (N. S.) 67, 1–92.

Newton, A. F., Thayer, M. K. 2005. Catalog of higher taxa, genera and subgenera of Staphyliniformia [online]. Chicago: Field Museum of Natural History [3 November 2005]. Available from URL: http://www.fieldmuseum.org/peet_staph/db_1a.html Accessed [11 August, 2015].

Nixon, K. C. 1999. WINCLADA (Beta), v. 0.z.9. – Software published by the author, Ithaca, New York. [online]. URL http:// www.cladistics.com.

O'Reilly, J. E., Puttick, M. N., Parry, L., Tanner, A. R., Tarver, J. E., Fleming, J., Pisani, D., Donoghue, P. C. J. 2016. Bayesian methods outperform parsimony but at the expense of precision in the estimation of phylogeny from discrete morphological data. Biol. Lett. 12, 1–5. http://dx.doi.org/10.1098/rsbl.2016.0081.

Parker, J. 2016. Myrmecophily in Beetles (Coleoptera): Evolutionary Patterns and Biological Mechanisms. Myrmecol. News 22, 65–108.

Rambaut, A., Suchard, M., Xie, D., Drummond, A. 2014. Tracer v1.6, available from http://beast.bio.ed.ac.uk/Tracer.

Reeder, T. W., Townsend, T. M., Mulcahy, D. G., Noonan, B. P., Wood, P. L. Jr., Sites, J. W. Jr., Wiens, J. J. 2015. Integrated Analyses Resolve Conflicts over Squamate Reptile Phylogeny and Reveal Unexpected Placements for Fossil Taxa. PLoS ONE 10, e0118199.

Robertson, J. A., Ślipiński, A., Hiatt, K., Miller, K. B., Whiting, M. F., McHugh, J. V. 2013. Molecules, morphology and minute hooded beetles: a phylogenetic study with implications for the evolution and classification of Corylophidae (Coleoptera: Cucujoidea). Syst. Entomol. 38, 209–232.

Ronquist, F., Teslenko, M., van der Mark, P., Ayres, D., Darling, A., Höhna, S., Larget, B., Liu, L., Suchard, M., Huelsenbeck, J. 2012. MrBayes 3.2: efficient Bayesian phylogenetic inference and model choice across a large model space. Syst. Biol. 61, 539–542.

Scheerpeltz, O. 1933. Staphylinidae VII. In: Schenkling, S. (Ed.), Coleopterorum Catalogus. Pars 129. W. Junk, Berlin, pp. 989–1500.

Scheerpeltz, O. 1962. Eine neue Gattung und Art der Tribus Quediini (Col. Staphylinidae). Ann. Nat. Hist. Mus. Wien. 65, 259–272.

Schillhammer, H. 1992. Six new Palaearctic species of the genus *Gabrius* Stephens and synonymical notes on some Philonthini. Koleopterol. Rundsch. 62, 61–67.

Schillhammer, H. 1997. Taxonomic revision of the Oriental species of *Gabrius* Stephens. Monographs on Coleoptera 1, 139 pp.

Schillhammer, H. 1998. Revision of the East Palaearctic and Oriental species of *Philonthus* Stephens - Part 1. The *cyanipennis* group. Koleopterol. Rundsch. 68, 101–118.

Schillhammer, H. 1999a. Revision of the East Palaearctic and Oriental species of *Philonthus* Stephens Part 2. The *spinipes* and *cinctulus* groups. Koleopterol. Rundsch. 69, 55–65.

Schillhammer, H. 1999b. Nomenclatoral changes in the subfamily Staphylininae (Coleoptera: Staphylinidae). Entomol. Probl. 30 (2), 93–95.

Schillhammer, H. 2000. Revision of the East Palaearctic and Oriental species of *Philonthus* Stephens Part 3. The *politus* complex. Koleopterol. Rundsch. 70, 113–176.

Schillhammer, H. 2001a. Revision of the East Palaearctic and Oriental species of *Philonthus* Stephens Part 4. The *amplitarsis* group and an additional species of the *cinctulus* group. Koleopterol. Rundsch. 71, 59–65.

Schillhammer, H. 2001b. Studies on the *Eucibdelus* lineage: 1. *Trichocosmetes* Kraatz, *Sphaeromacrops* gen.n., *Guillaumius* gen.n., and *Rhyncocheilus* Sharp. - Koleopterol. Rundsch. 71, 67–96.

Schillhammer, H. 2001c. The Taiwan species of *Gabrius* Stephens. Ann. Nat. Hist. Mus. Wien, 103 B, 391–411.

Schillhammer, H. 2002. Three new species of *Hesperus* Fauvel from South-east Asia. Koleopterol. Rundsch. 72, 127–135.

Schillhammer, H. 2003. Revision of the East Palaearctic and Oriental species of *Philonthus* Stephens Part 5. The *rotundicollis* and *sanguinolentus* species groups. Koleopterol. Rundsch. 73, 85–136.

Schillhammer, H. 2004a. Studies on the *Eucibdelus* lineage. 2. New species of *Rhynocheilus* Fauvel and *Phytolinus* Sharp. Koleopterol. Rundsch. 74, 245–250.

Schillhammer, H. 2004b. Critical notes on the subtribe Anisolinina with descriptions of nine new species. Koleopterol. Rundsch. 74, 251–277.

Schillhammer, H. 2006. Revision of the genus *Algon* Sharp. Koleopterol. Rundsch. 76, 135–218.

Schillhammer, H. 2008. New species and records of *Algon* Sharp. Koleopterol. Rundsch. 78, 233–240.

Schillhammer, H. 2011. Old and new Staphylinini from the Palearctic and Oriental regions. Koleopterol. Rundsch. 81, 133–163.

Schillhammer, H. 2016. *Hesperus rougemonti* sp. n. (Coleoptera, Staphylinidae) from Borneo. Zootaxa 4061(2), 197.

Schillhammer, H., Snäll, S., Coskun, M., Jansson, N. 2007. The West Palearctic species of *Hesperus* Fauvel, 1874, with descriptions of three new species from Turkey. Koleopterol. Rundsch. 77, 123–132.

Seevers, C. H. 1965. The systematics, evolution and zoogeography of staphylinid beetles associated with army ants (Coleoptera, Staphylinidae). Fieldiana, Zoology 47(2), 139–351.

Sereno, P. C. 2007. Logical basis for morphological characters in phylogenetics. Cladistics 23, 565–587.

Sereno, P. C. 2009. Comparative cladistics. Cladistics 25, 624–659.

Sharp, D. S. 1874. The Staphylinidae of Japan. Trans. R. Entomol. Soc. Lond. 1874, 1–103.

Sharp, D. S. 1885. Staphylinidae. Pp. 393–536. In: Biologia Centrali-Americana. Insecta. Coleoptera. 1(2). London: Taylor & Francis.

Sharp, D. S. 1889. The Staphylinidae of Japan. Ann. Mag. Nat. Hist. (6), 3, 108–121.

Simmons, M., Randle, C. 2014. Disparate parametric branch-support values from ambiguous characters. Mol. Phylogenet. Evol. 78, 66–86.

Smetana, A. 1977. The Nearctic genus *Beeria* Hatch. Taxonomy, distribution and ecology (Coleoptera: Staphylinidae). Entomol. Scand. 8, 177–190.

Smetana, A. 1988. Revision of the tribes Quediini and Atanygnathini. Part II. The Himalayan Region (Coleoptera: Staphylinidae). Quaest. Entomol., 24, 163-464.

Smetana, A. 1995. Rove beetles of the subtribe Philonthina of America north of Mexico (Coleoptera:

Staphylinidae): Classification, phylogeny and taxonomic revision. Memoirs on Entomology, International 3, 1–946.

Smetana, A., Davies, A. 2000. Reclassification of the North Temperate Taxa Associated with *Staphylinus* Sensu Lato, Including Comments on Relevant Subtribes of Staphylinini (Coleoptera: Staphylinidae). Am. Mus. Nov. 3287, 1–88.

Solodovnikov, A. 2005. *Natalignathus*, gen. nov. and larvae of *Atanygnathus*: a missing phylogenetic link between subtribes Quediina and Tanygnathinina (Coleoptera: Staphylinidae: Staphylininae: Staphylinini). Invertebr. Syst. 19, 75–98.

Solodovnikov, A. Y. 2006. Revision and phylogenetic assessment of *Afroquedius* gen. nov. from South Africa: toward new concepts of the genus *Quedius*, subtribe Quediina and reclassification of the tribe Staphylinini (Coleoptera: Staphylinidae: Staphylininae). Ann. Entomol. Soc. Am. 99, 1065–1084.

Solodovnikov, A. 2012. Rove beetle subtribes Quediina, Amblyopinina and Tanygnathinina: systematic changes affecting Central European fauna (Coleoptera, Staphylinidae, Staphylinini). ZooKeys 162, 25–42.

Solodovnikov, A., Brunke, A. 2016. *Cafioquedus gularis* Sharp, 1886 and other poorly understood Staphylinini: a review of the New Zealand fauna of the tribe with discussion of its potential for biogeography (Insecta: Coleoptera: Staphylinidae). New Zeal. Entomol. 39(1), 40–61.

Solodovnikov, A., Newton, A. 2005. Phylogenetic placement of Arrowinini trib.n. within the subfamily Staphylininae (Coleoptera: Staphylinidae), with revision of the relict South African genus *Arrowinus* and description of its larva. Syst. Entomol. 30, 398–441.

Solodovnikov, A., Schomann, A. 2009. Revised systematics and biogeography of 'Quediina' of sub-Saharan Africa: new phylogenetic insights into the rove beetle tribe Staphylinini (Coleoptera: Staphylinidae). Syst. Entomol. 34, 443–466.

Solodovnikov, A., Yue, Y., Tarasov, S., Ren, D. 2013. Extinct and extant rove beetles meet in the matrix: Early Cretaceous fossils shed light on the evolution of a hyperdiverse insect lineage (Coleoptera: Staphylinidae: Staphylininae). Cladistics 29, 360–403.

Sørensen, M. V., Dal Zotto, M., Rho, H. S., Herranz, M., Sánchez, N., Pardos, F., *et al.* 2015. Phylogeny of Kinorhyncha Based on Morphology and Two Molecular Loci. PLoS ONE 10(7), e0133440.

Talavera, G., Castresana, J. 2007. Improvement of phylogenies after removing divergent and ambiguously aligned blocks from protein sequence alignments. Syst. Biol. 56, 564–577

Wiens, J. J. 2004. The role of morphological data in phylogeny reconstruction. Syst. Biol. 53, 653–661.

Wiens, J. J. 2005. Can incomplete taxa rescue phylogenetic analyses from long-branch attraction? Syst. Biol. 54, 731–742.

Wiens, J. J. 2009. Paleontology, phylogenomics, and combined-data phylogenetics: can molecular data improve phylogeny estimation for fossil taxa? Syst. Biol. 58, 87–99.

Wild, A. L., Maddison, D. R. 2008. Evaluating nuclear protein-coding genes for phylogenetic utility in beetles. Mol. Phylogenet. Evol. 48, 877–891.

Table Caption

Tables 1-2. Molecular and morphological synapomorphies in support of major lineages at subtribal (Table 1) and genus level (Table 2) optimized in TNT on the greatest likelihood topology (ML) and the 23 MPTs (PEW). Molecular synapomorphies shown in number of base pairs per gene fragment (WG, 28s, ArgK, COI, Topo, CAD C, CAD A). Loci with the most synapomorphies/node are **bold**, those without

synapomorphies are indicated with (-), and those where synapomorphies could not be estimated due to missing data are indicated with (--). Abbreviations: (N) synapomorphies not informed by TNT; */** synapomorphies optimized in TNT on the three MPTs from PIW (K=7).
Abbreviations: PEW, Maximum parsimony under equal weights; PIW, Maximum parsimony under implied weights.

Figure Captions

Figure 1. Fifty per cent majority rule consensus tree from a partitioned Bayesian analysis of a combined dataset of 4571 characters (4458 DNA, 113 morphology). Posterior probabilities (PP) greater than 0.81 reported to the left of the corresponding node: above (PP from all taxa dataset); below (PP, if improved after using only taxa with DNA available). Five terminal taxa with no available DNA (*). Abbreviations: ASA= Austral South America, Au= Australia, NA= Nearctic, NT= Neotropical, NZ= New Zealand, Or= Oriental, PA= Palearctic, S Afr= South Africa; BI=Bayesian, ML= Maximum Likelihood; P= Parsimony.

Figure 2. Topological congruence between: (A) greatest likelihood topology recovered by partitioned maximum likelihood analysis and (B) strict consensus topology of 23 most parsimonious trees recovered by Maximum Parsimony under equal weights using TNT. Nodes with Bootstrap (A) or jackknife (B) values greater than 50 reported to the right of their corresponding node.

Figure 3. Morphological characters mapped onto the greatest likelihood topology recovered by partitioned maximum likelihood analysis. Filled circles: exclusive synapomorphies; empty circles: non-exclusive synapomorphies.

Figure 4. A) Strict consensus topology (70 most parsimonious trees) recovered by Maximum Parsimony under equal weights using TNT for the morphological dataset (135 taxa, 113 characters) with jackknife values greater than 50 reported to the left of their corresponding node. B) Fifty per cent majority rule consensus tree from a partitioned Bayesian analysis of the molecular dataset (133 taxa, 4458 bp) with colored nodes indicating support.

Figure 5. Morphological diversity of ‘Staphylinini propria’ subtribes after the present study, except Philonthina.

Figure 6. Morphological diversity of Philonthina and Hyptiomina after the present study.

Figure 7. *Algon reuteri* Schillhammer: median lobe with “operculum”. Scale bar: 0.5 mm.

Figure 8. *Philothalpus brooksi* Chatzimanolis and Ashe: A) Prosternum and mesoventrite (part), B) Abdominal tergites 3-5, accessory ridges on anterior basal tranverse carina. Abbreviations: bs, basisternum; fs, furcasternum; r(la), mesoventral ridge (lateral arm); sts, sternopleural (anapleural) suture.

Supporting information

1) Tables S1 and S2. Taxon sampling and genes.
2) Morphological matrix (Mesquite)
3) Combined matrix (for Mr. Bayes)
4) Strict consensus topology (12 most parsimonious trees) recovered by Maximum Parsimony under equal weights using TNT for the combined dataset, excluding representatives of Tanygnathinina. Jackknife values greater than 50 reported to the left of their corresponding node.

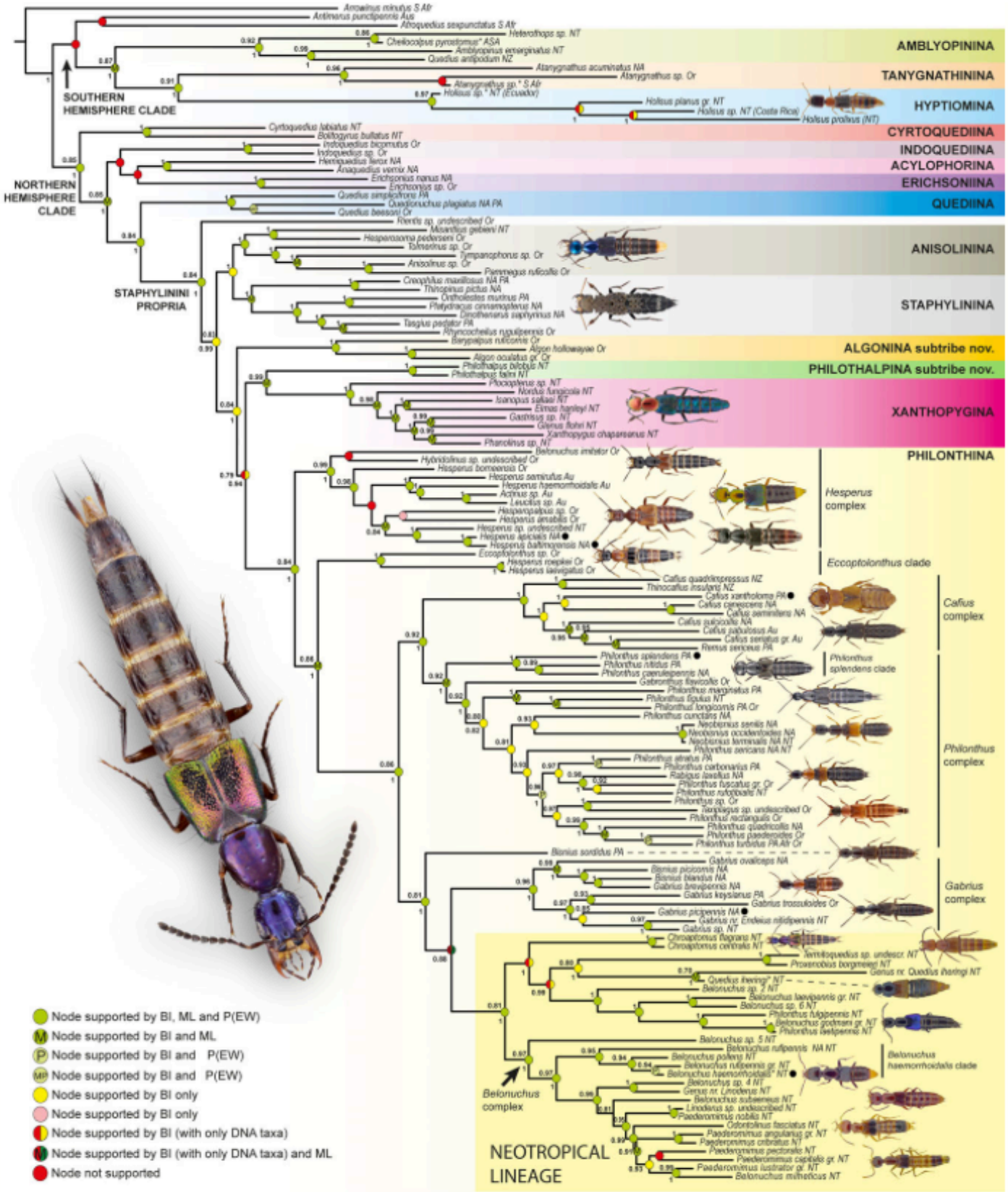

Fig. 1. Fifty per cent majority rule consensus tree from a partitioned Bayesian analysis of a combined dataset of 4571 characters (4458 DNA, 113 morphology). Posterior probabilities (PP) of greater than 0.81 are reported to the left of the corresponding node: above (PP from all taxa dataset); below (PP, if improved after using only taxa with DNA available). Type species of genera or close relatives are marked by filled black circles. *Five terminal taxa with no available DNA. Abbreviations: ASA, Austral South America; Au, Australia; NA, Nearctic; NT, Neotropical; NZ, New Zealand; Or, Oriental; PA, Palearctic; S Afr, South Africa; BI, Bayesian; ML, maximum likelihood; P, parsimony.

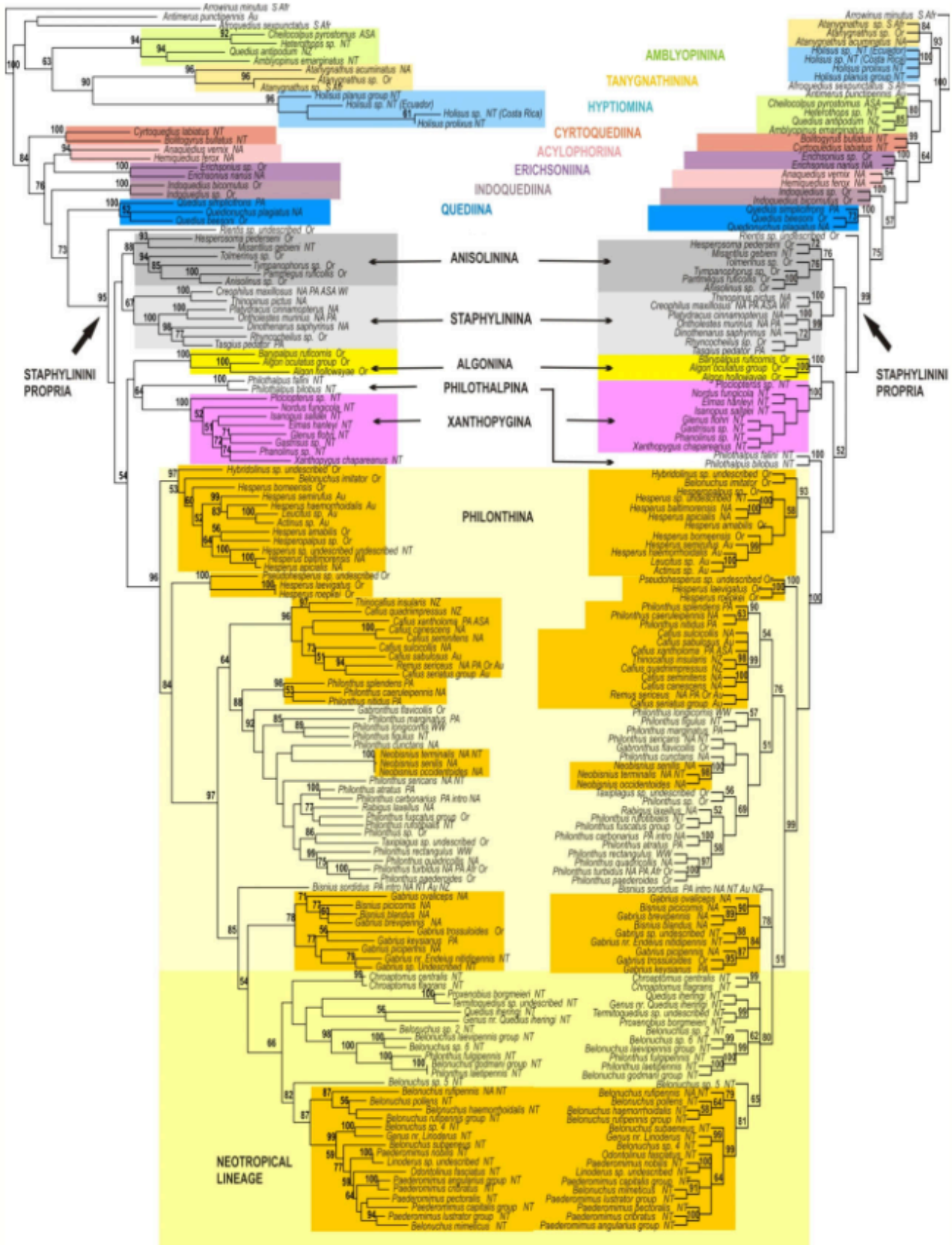

Fig. 2. Topological congruence between: (A) greatest likelihood topology recovered by partitioned maximum likelihood analysis and (B) strict consensus topology of 23 most parsimonious trees recovered by maximum parsimony under equal weights using TNT. Nodes with bootstrap (A) or jackknife (B) values greater than 50 are reported to the right of their corresponding node.

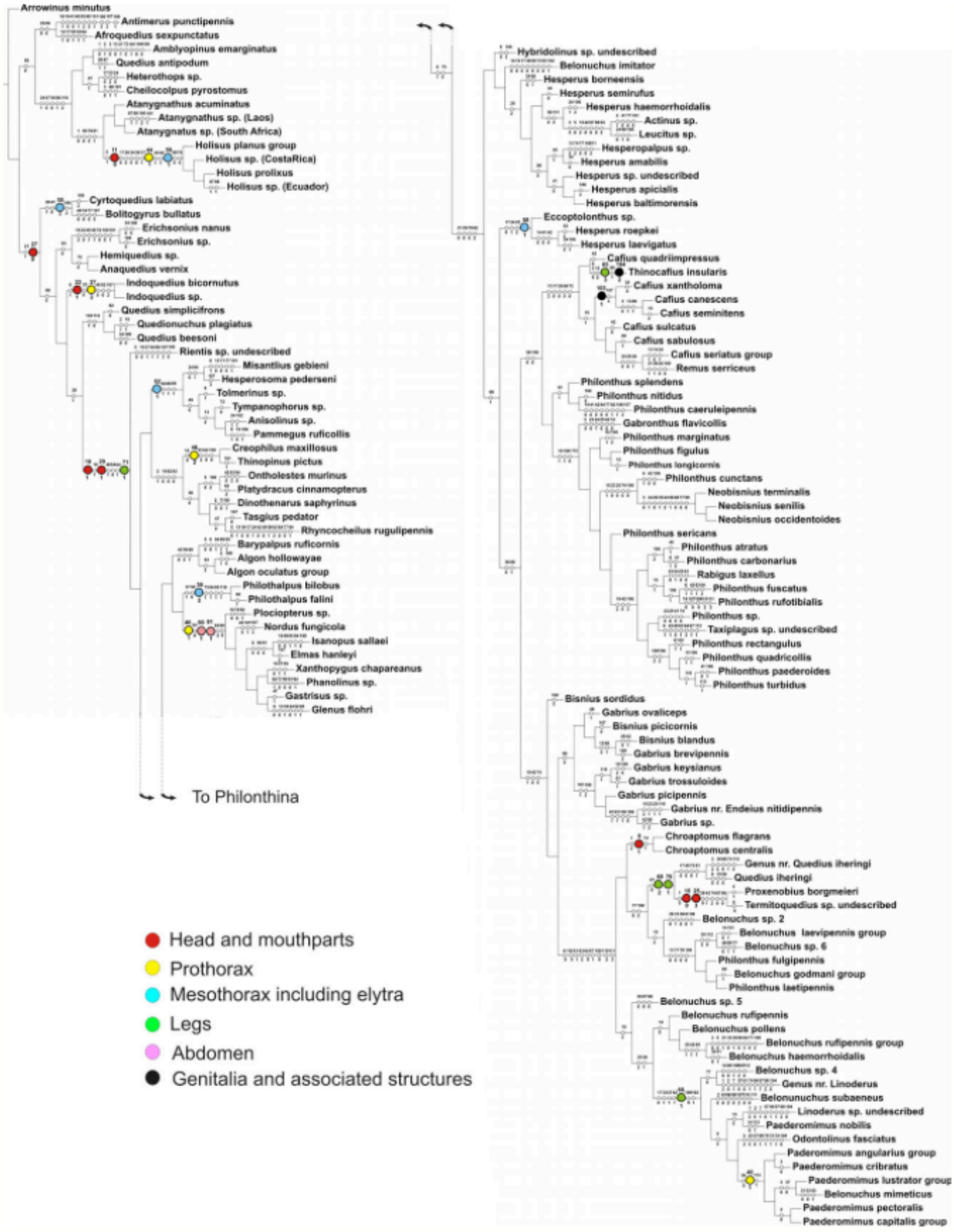

Fig. 3. Morphological characters mapped onto the greatest likelihood topology recovered by partitioned maximum likelihood analysis. Filled circles: exclusive synapomorphies; empty circles: non-exclusive synapomorphies.

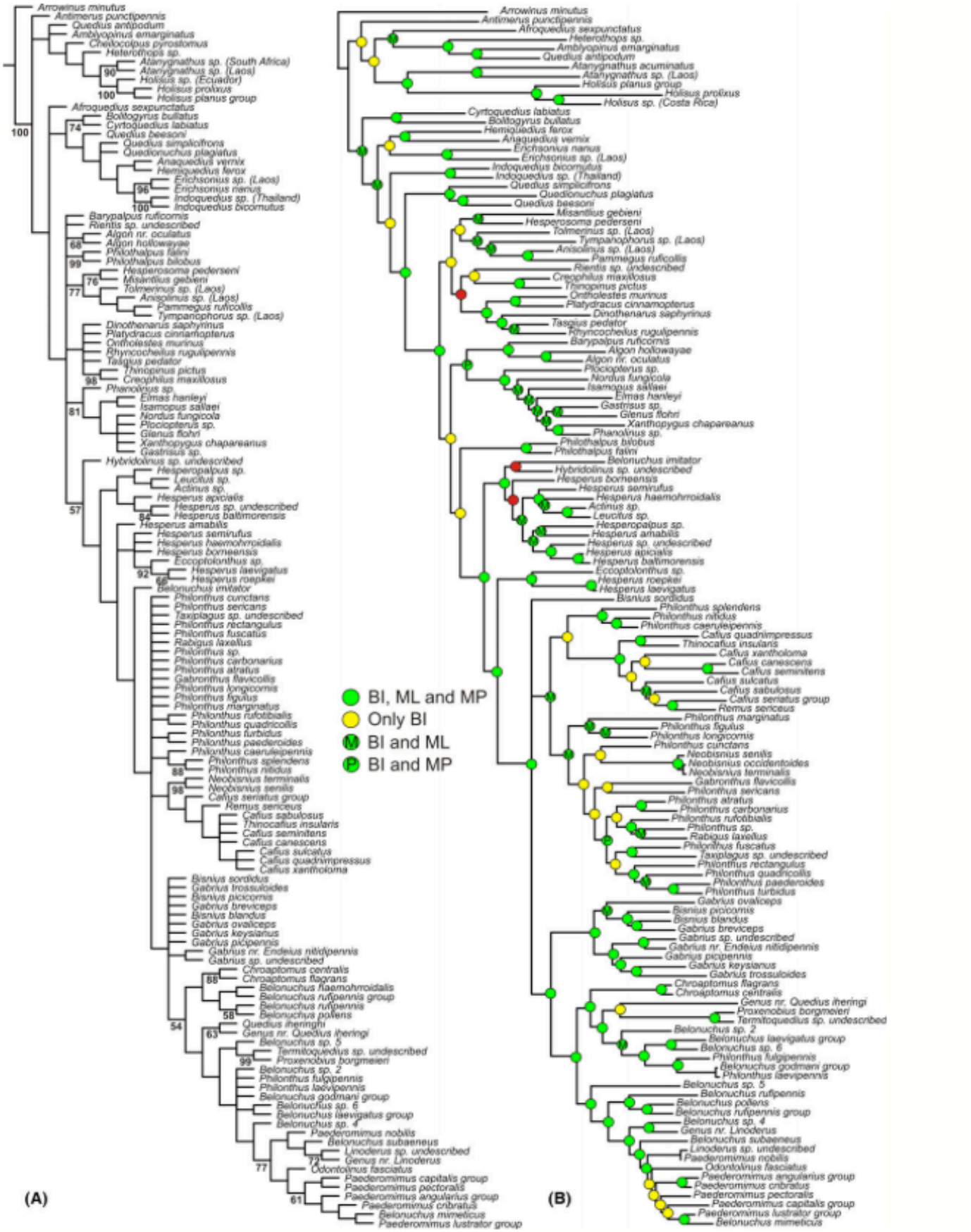

Fig. 4. (A) Strict consensus topology (70 most parsimonious trees) recovered by maximum parsimony under equal weights using TNT for the morphological dataset (135 taxa, 113 characters) with jackknife values > 50 reported to the left of their corresponding node. (B) Fifty per cent majority rule consensus tree from a partitioned Bayesian analysis of the molecular dataset (133 taxa, 4458 bp) with coloured nodes indicating support.

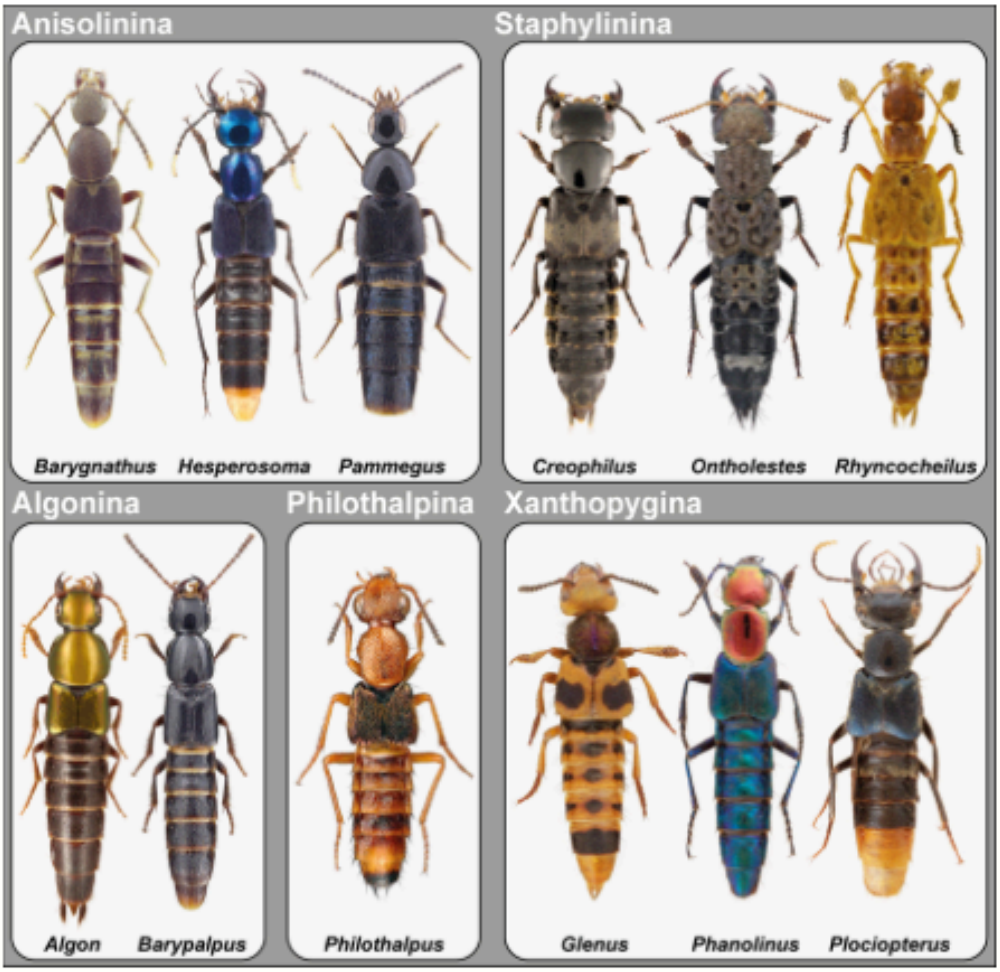

Fig. 5. Morphological diversity of 'Staphylinini propria' subtribes after the present study, except Philonthina.

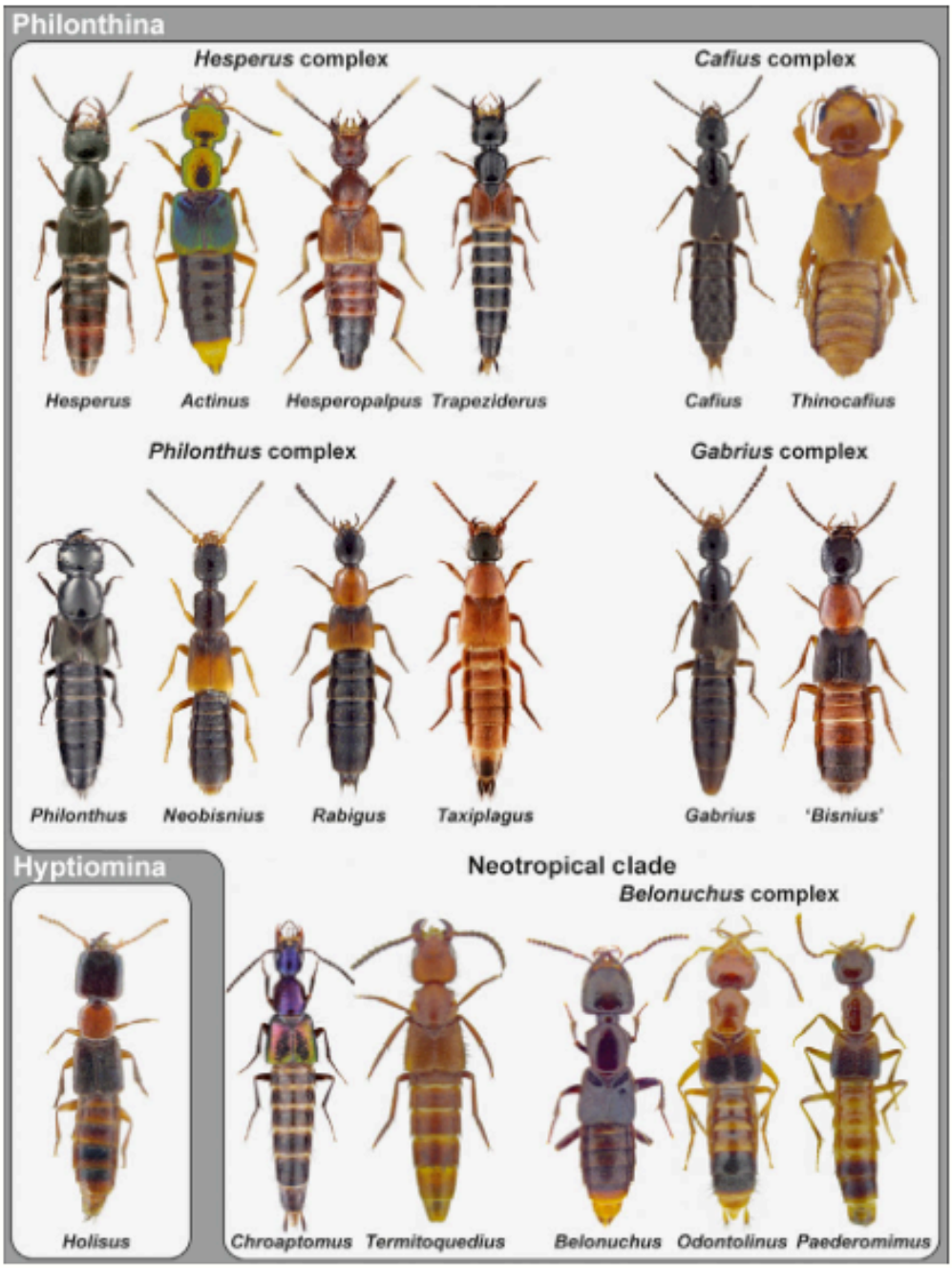

Fig. 6. Morphological diversity of Philonthina and Hyptiomina after the present study.

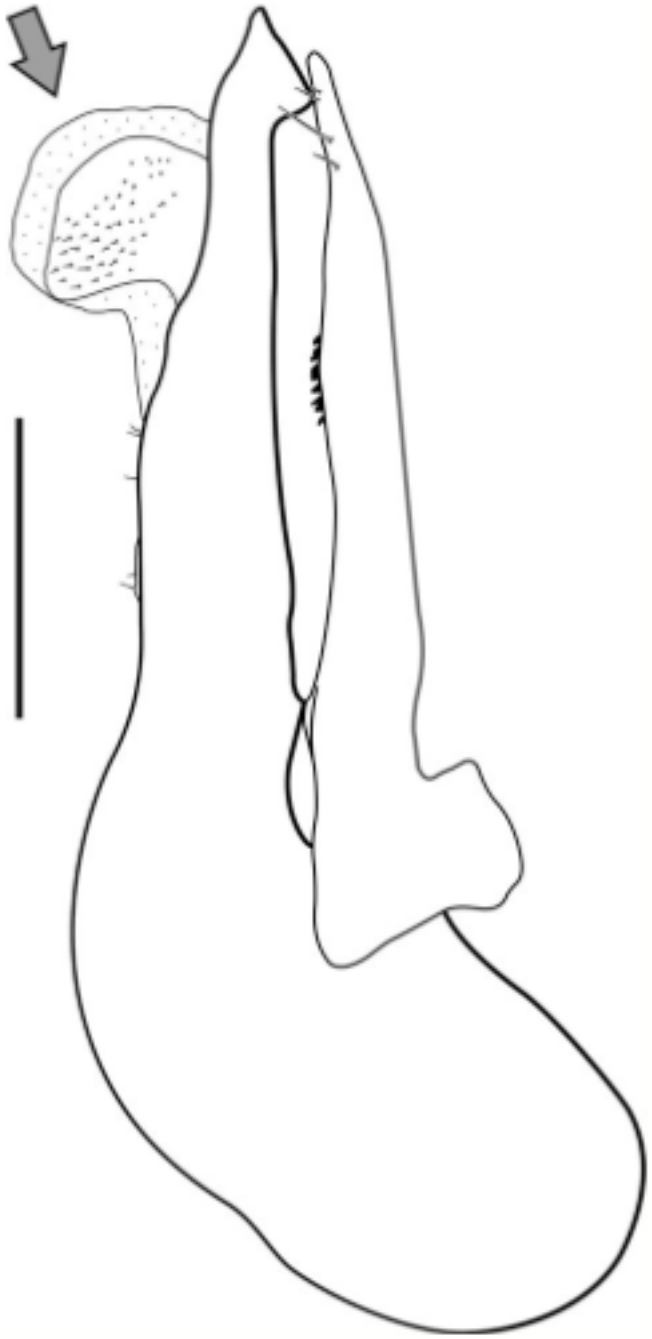

Fig. 7. *Algon reuteri* Schillhammer: median lobe with 'operculum'. Scale bar: 0.5 mm.

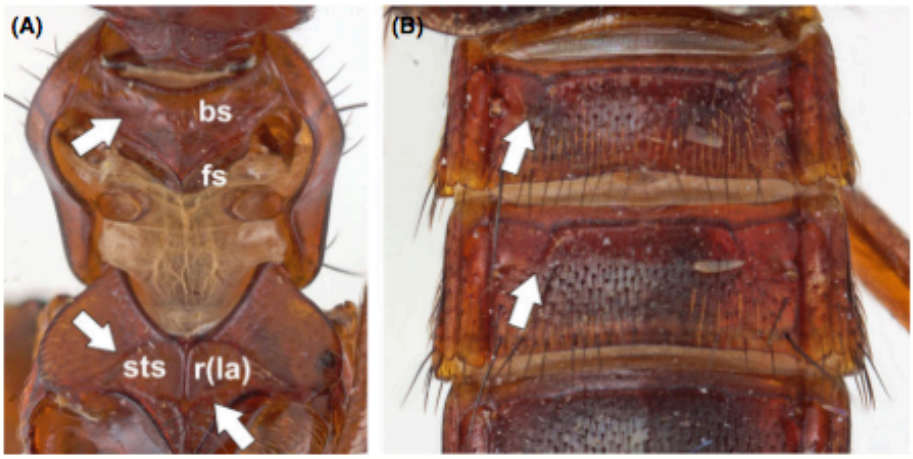

Fig. 8. *Philothalpus brooksi* Chatzimanolis and Ashe: (A) prosternum and mesoventrite (part), (B) abdominal tergites 3–5, accessory ridges on anterior basal tranverse carina. Abbreviations: bs, basisternum; fs, furcasternum; r(la), mesoventral ridge (lateral arm); sts, sternopleural (anapleural) suture.

Table 1
Molecular and morphological synapomorphies in support of major lineages at subtribal level optimized in TNT on the greatest likelihood topology (ML) and the 23 MPTs (PEW)

Clades – subtribal level Synapomorphies	Σ synapo/ 4571		WG – 388		28s – 622		COI – 793		ArgK – 708		Topo – 684		CAD C – 645		CAD A – 618		Morph – 113		List of morphological synapomorphies **ML and MP**, MP or *ML* only
	ML	P	ML	P	ML	P	ML	P	ML	P	ML	P	ML	P	ML	P	ML	P	
Amblyopinina	N	78	N	15	–	–	N	7	N	12	N	**25**	N	–	N	13	N	6	24(1), 53(0), 54(0) 80(1), 110(2), 111(1)
Acylophorina	56	55	2	3	2	2	8	12	**14**	**15**	9	9	9	5	11	8	1	1	**75(0)**
Anisolinina	25	24	–	–	–	–	3	3	2	2	**12**	**9**	–	–	4	6	4	4	**2(1), 19(0), 82(0), 93(0)**
Barypalpus + *Algon*	56	53	9	8	**18**	**15**	8	6	6	8	12	13	–	–	–	–	3	3	**42(0), 56(0), 68(1)**
Cyrtoquediina	71	70	1	–	6	6	10	8	12	14	10	14	10	9	**18**	**16**	4	3	**20(1)**, *41(0)*, **55(1), 100(2)**
Erichsoniina	74	75	11	10	13	13	17	21	–	–	**26**	**23**	–	–	–	–	7	8	**18(2), 25(0), 45(1), 48(1), 78(0), 100(0), 101(1),** 112(0)
Hyptiomina	68	11	1	–	1	–	8	–	2	–	**32**	–	6	–	5	–	13	11	*2(1)*, **11(0), 17(0), 26(0), 34(0), 36(0), 37(1), 44(1), 45(1), 48(1), 59(1)**, *68(0)*, **78(0)**
Hyptiomina + Tanygnathinina	64	73	4	5	6	6	7	6	9	11	14	16	**15**	**17**	5	6	4	6	**1(0)**, 49(0), 51(0), **69(0), 70(0), 81(1)**
Indoquediina	61	68	6	7	–	–	13	15	13	14	–	–	–	–	**22**	**24**	7	8	**6(1), 22(1), 25(0), 37(2), 49(0), 82(0),** 106(0), **107(2)**
Philonthina	54	54	4	3	8	8	6	2	5	2	**15**	**18**	5	7	7	8	4	6	**21(0), 29(0),** 45(1), **78(0), 82(2),** 85(1)
Philonthina – Neotropical clade	55	31	6	3	7	6	1	–	6	5	**11**	6	10	–	5	**7**	9	4	*41(0), 50(0), 61(1), 63(2),* **64(0)**, *67(1)*, **109(0), 110(2), 111(2)**
Quediina	82	85	7	8	6	6	7	7	8	8	**22**	**21**	15	18	15	15	2	2	**102(1), 112(0)**
Quediina + Staphylinini propria	50	51	2	2	–	–	3	4	5	6	12	13	**18**	**16**	9	9	1	1	**20(1)**
Staphylinina*	31	27	–	–	1	1	3	2	2	2	**7**	**7**	**7**	5	**7**	6	4	4	**2(1), 19(0), 82(0), 93(0)**
Staphylinini northern clade	46	32	4	3	1	1	2	4	6	2	**16**	**9**	8	8	7	3	2	2	**21(1), 27(0)**
Staphylinini propria (*Rientis* included)	64	64	5	3	6	6	10	11	12	12	**14**	**16**	–	–	10	9	7	7	**10(1), 16(1), 29(1), 48(1), 54(0), 64(1), 71(1)**
Tanygnathinina	135	137	15	11	13	17	15	16	27	23	16	18	**29**	**29**	20	17	–	6	3(0), 4(1), 19(2), 42(0), 65(0), 111(1)
Xanthopygina	92	85	6	7	8	5	9	8	11	8	**23**	**23**	13	14	16	13	6	7	30(1), **46(1), 64(0), 90(1), 91(1), 93(2), 99(0)**
Xanthopygina + *Philothalpus* †	40	33	–	1	–	–	3	4	9	4	8	4	**13**	**11**	7	9	–	–	
Total	1123	1054	83	89	96	92	133	136	149	148	**259**	**244**	158	139	168	169	78	89	

*Recovered unsupported by PEW and PIW (all K values).
†Not recovered by PEW, but recovered unsupported by PIW (all K values).

Table 2
Molecular and morphological synapomorphies in support of major lineages at genus level optimized in TNT on the greatest likelihood topology (ML) and the 23 MPTs (PEW)

Synapomorphies	Σ synapo/ 4571		WG – 388		28s – 622		COI – 793		ArgK – 708		Topo – 684		CAD C – 645		CAD A – 618		Morph – 113		List of morphological synapomorphies **ML and MP**, MP or *ML* only
	ML	P	ML	P	ML	P	ML	P	ML	P	ML	P	ML	P	ML	P	ML	P	
Belonuchus-complex	43	29	9	6	3	1	5	2	3	3	9	5	**12**	10	–	–	2	2	**25(2), 38(1)**
Belonuchus haemorrhoidalis clade	37	30	5	4	8	7	8	5	3	2	–	–	–	–	**12**	**11**	1	1	**14(0)**
Cafius clade (*Thinocafius* and *Remus* included)	99	85	5	8	1	2	1	–	4	2	21	16	**31**	25	**31**	**28**	5	4	*13(2)*, **17(0), 26(0), 68(0), 72(0)**
Chroaptomus	100	73	14	6	–	–	**45**	**33**	16	14	22	18	–	–	–	–	3	2	**1(2), 8(1)**, *74(1)*
Eccoptolonthus clade	76	69	5	3	2	1	10	8	9	10	17	14	**18**	**18**	11	11	4	4	**17(0), 24(1), 25(2), 58(1)**
Gabrius clade (*B. blandus* and *B. picicornis* included)	77	12	7	**7**	2	2	6	2	10	–	17	–	**22**	–	12	–	1	1	**99(0)**
Hesperus-complex (*Belonuchus imitator, Hybridolinus, Actinus, Leucitus* and *Hesperopalpus* included)	15	38			2	2	7	3	6	6	–	**13**	–	1	–	12		1	63(2)
Neobisnius	52	49	15	**16**	11	9	–	–	**17**	15	–	–	–	–	–	–	9	9	**3(0), 24(1), 26(0), 26(0), 35(1), 43(2), 56(1), 68(0), 77(0), 99(0)**
Paederomimus subclade (excluding *P. nobilis* and including *Belonuchus mimeticus*)*	13	12	3	1	3	2	**4**		–	3	–	3	–	–	–	3	3	–	**36(0), 40(1), 113(1)**
Philonthus splendens clade	65	65	4	6	–	–	17	15	1	–	**18**	**20**	11	9	13	14	1	1	15(2), **61(1)**
Philonthus complex (all *Philonthus* representatives except two in the NT lineage *Gabronthus, Neobisnius, Rabigus* and *Taxiplagus* included)*	31	27	**9**	5	1	1	2	4	4	4	8	**8**	3	3	4	1		1	26(1)
Philothalpus	66	63	5	2	3	–	**27**	26	–	–	–	–	–	–	24	**29**	7	6	**37(1), 50(0), 56(2)**, *75(1)*, **84(1), 95(1)**, 106(2), *110(1)*
Total	674	552	81	64	36	27	**132**	98	73	59	112	97	97	66	107	**109**	36	32	

*Not recovered by PEW, but recovered from weakly to moderately supported by PIW (K = 6–12).